Pumping the Brakes on Pulmonary Fibrosis: A New Role for Regulator of Cell Cycle

As a result of injury or damage, tissue fibrosis can occur in any organ throughout the body. Within the lungs, there is a robust repair response initiated through a variety of different physiological mechanisms. Although the wound healing response is necessary to preserve lung function, the repair process can go awry, resulting in fibrosis, which is defined as the accumulation of excessive extracellular matrix protein or fibrous connective tissue. The most severe form is termed idiopathic pulmonary fibrosis (IPF), which causes shortness of breath, respiratory distress, and ultimately death. There are several U.S. Food and Drug Administration–approved therapies for pulmonary fibrosis that delay disease progression, but currently there is no cure. One reason for the lack of therapeutic options is that fibrosis is a multicellular event that begins with injury to the epithelial cells, leads to recruitment and/or stimulation of the immune system, and results in the activation and differentiation of fibroblasts (1). Because of the complexity of these signaling pathways and cell-to-cell interactions, identification and characterization of molecular brakes are needed to halt or possibly reverse the damage caused by excessive collagen secretion and remodeling. The development of novel strategies to restore these braking mechanisms may halt the disease progression and allow the lung time to repair and reverse the disease process.

In this issue of the *Journal*, Luzina and colleagues (pp. 146–157) report that the protein RGCC (regulator of cell cycle) is a novel suppressor of fibrotic signaling in fibroblasts (2). The authors demonstrate that expression of RGCC in whole lung tissue isolated from both murine models of pulmonary fibrosis and patients with IPF was decreased when compared with normal, donor controls. Although RGCC is expressed in various cells throughout the lung, the decrease in fibroblasts was most pronounced, leading the investigators to focus on the role of this protein in that cell population. Interestingly, mice deficient in RGCC had paradoxical reactions to bleomycin-induced pulmonary fibrosis with reduced collagen production when challenged with one dose of bleomycin and elevated collagen when challenged with multiple doses, inducing a chronic fibrotic model. Using primary human lung fibroblasts, the authors show that overexpression of RGCC attenuates TGF-β (transforming growth factor-β) activation of fibroblasts by inhibiting Smad signaling. This study confirms that fibrosis is associated with diminished RGCC expression and broad, diminished antifibrotic effects in fibroblasts.

Although originally identified within the central nervous system, RGCC is abundantly expressed throughout the body and has a role in many fundamental biological processes, including cell proliferation and differentiation, tumorigenesis, innate and adaptive immunity, and fibrosis (3). The first description of RGCC in fibrosis was in a murine model of kidney injury and repair (4). In this model, RGCC was elevated early after injury and inhibition by shRNA resulted in reduced collagen deposition and α-SMA (α-smooth muscle actin expression), as a marker of fibroblast activation. More recently, investigators examined the role of RGCC in skin fibrosis and inflammation using a bleomycin-induced systemic sclerosis murine model (5). RGCC-deficient mice had reduced skin thickening, fibrosis, and decreased collagen deposition, as well as diminished macrophage infiltration and proinflammatory cytokine production. Interestingly, other reports have demonstrated that RGCC expression is dependent on the response to both profibrotic factors, such as TGF-β, and proinflammatory cytokines, such as TNF-α (6). Given the role of this pleotropic protein in regulating the cell cycle, inflammatory signaling, and fibrotic pathways, additional work is needed to investigate RGCC in injury and repair responses in different tissues.

To extend the current study and further assess the role of RGCC in pulmonary fibrosis, it is important to consider the issue of fibroblast heterogeneity within the lung microenvironment. Recent studies using animal models have demonstrated the presence of fibroblast subtypes across a variety of different organs (7). Within the human lung, single-cell RNA sequencing analysis of lung tissue from IPF or normal donor controls has identified distinct fibroblast subpopulations (8, 9). In this study, the authors examine RGCC expression using both human and animal models. Although whole lung samples from the murine models consistently demonstrate diminished RGCC expression after bleomycin challenge, human lung fibroblasts exhibit considerably more heterogeneity in their protein expression of RCGG. These issues could be related to differences in RGCC expression between species (mouse vs. human), types of samples (whole lung vs. isolated cells), or fibroblast subtypes. The question going forward is to how to align expression and functional data of specific proteins with the possibility of fibroblast heterogeneity within the lung microenvironment.

Given the high clinical significance of myofibroblast dedifferentiation studies, additional work evaluating the effect of RGCC in Smad-independent pathways would be worth pursuing. In a recent study published by Fortier and colleagues, RNA sequencing analysis revealed that RGCC was upregulated by dedifferentiation agents, such as prostaglandin E_2 and fibroblast growth factor 2, indicating a likely role for this protein in mediating the dedifferentiation process (10). Therefore, RGCC induction responses to dedifferentiation agents and the ability to signal through RGCC-dependent pathways are needed to better understand this protein's pleiotropic actions. Another characteristic feature of fibrotic fibroblasts is their notorious resistance to apoptosis (11). Although RGCC has not been studied extensively in this context, one study reported that loss of RGCC promotes cell survival in nerve cells (12), suggesting a possible role for this protein in apoptosis resistance.

Taken together, these results provide a strong foundation suggesting that the loss of RGCC in fibroblasts contributes to

Originally Published in Press as DOI: 10.1165/rcmb.2021-0399ED on November 10, 2021

pulmonary fibrosis. Using murine models of pulmonary fibrosis and primary human lung fibroblasts isolated from patients with and without fibrosis, the authors demonstrate that RGCC regulates expression of collagen and α-SMA as well as extracellular collagen deposition. Additional studies are necessary to explore the mechanism by which RGCC regulates fibrotic signaling pathways. These studies provide an important launching point to investigate further biological effects of this protein in regulating cell proliferation and proinflammatory and profibrotic pathways. ■

Author disclosures are available with the text of this article at www.atsjournals.org.

Loka Raghu Kumar Penke, Ph.D.
Department of Internal Medicine
University of Michigan
Ann Arbor, Michigan

Gina Torres Matias, Ph.D.
Megan N. Ballinger, Ph.D.
Department of Internal Medicine
The Ohio State University Wexner College of Medicine
Columbus, Ohio

ORCID IDs: 0000-0002-2780-7950 (L.R.K.P.); 0000-0002-2202-3049 (M.N.B.).

References

1. Henderson NC, Rieder F, Wynn TA. Fibrosis: from mechanisms to medicines. *Nature* 2020;587:555–566.
2. Luzina IG, Rus V, Lockatell V, Courneya JP, Hampton BS, Fishelevich R, *et al.* Regulator of cell cycle protein (RGCC/RGC-32) protects against pulmonary fibrosis. *Am J Respir Cell Mol Biol* 2022;66:146–157.
3. Vlaicu SI, Tatomir A, Anselmo F, Boodhoo D, Chira R, Rus V, *et al.* RGC-32 and diseases: the first 20 years. *Immunol Res* 2019;67: 267–279.
4. Li Z, Xie WB, Escano CS, Asico LD, Xie Q, Jose PA, *et al.* Response gene to complement 32 is essential for fibroblast activation in renal fibrosis. *J Biol Chem* 2011;286:41323–41330.
5. Sun C, Chen SY. RGC32 promotes bleomycin-induced systemic sclerosis in a murine disease model by modulating classically activated macrophage function. *J Immunol* 2018;200:2777–2785.
6. Shen YL, Liu HJ, Sun L, Niu XL, Kuang XY, Wang P, *et al.* Response gene to complement 32 regulates the G2/M phase checkpoint during renal tubular epithelial cell repair. *Cell Mol Biol Lett* 2016; 21:19.
7. Muhl L, Genové G, Leptidis S, Liu J, He L, Mocci G, *et al.* Single-cell analysis uncovers fibroblast heterogeneity and criteria for fibroblast and mural cell identification and discrimination. *Nat Commun* 2020;11:3953.
8. Adams TS, Schupp JC, Poli S, Ayaub EA, Neumark N, Ahangari F, *et al.* Single-cell RNA-seq reveals ectopic and aberrant lung-resident cell populations in idiopathic pulmonary fibrosis. *Sci Adv* 2020;6:eaba1983.
9. Habermann AC, Gutierrez AJ, Bui LT, Yahn SL, Winters NI, Calvi CL, *et al.* Single-cell RNA sequencing reveals profibrotic roles of distinct epithelial and mesenchymal lineages in pulmonary fibrosis. *Sci Adv* 2020;6:eaba1972.
10. Fortier SM, Penke LR, King D, Pham TX, Ligresti G, Peters-Golden M. Myofibroblast dedifferentiation proceeds via distinct transcriptomic and phenotypic transitions. *JCI Insight* 2021;6:e144799.
11. Bühling F, Wille A, Röcken C, Wiesner O, Baier A, Meinecke I, *et al.* Altered expression of membrane-bound and soluble CD95/Fas contributes to the resistance of fibrotic lung fibroblasts to FasL induced apoptosis. *Respir Res* 2005;6:37.
12. Counts SE, Mufson EJ. Regulator of cell cycle (RGCC) expression during the progression of Alzheimer's disease. *Cell Transplant* 2017; 26:693–702.

ORIGINAL RESEARCH

Regulator of Cell Cycle Protein (RGCC/RGC-32) Protects against Pulmonary Fibrosis

Irina G. Luzina[1,2], Violeta Rus[1,2], Virginia Lockatell[1,2], Jean-Paul Courneya[3], Brian S. Hampton[1], Rita Fishelevich[1,2], Alexander V. Misharin[4], Nevins W. Todd[1,2], Tudor C. Badea[5,6], Horea Rus[1,2], and Sergei P. Atamas[1,2]

[1]University of Maryland School of Medicine, Baltimore, Maryland; [2]Baltimore VA Medical Center, Baltimore, Maryland; [3]Health Sciences and Human Services Library, University of Maryland–Baltimore, Baltimore, Maryland; [4]Division of Pulmonary and Critical Care Medicine, Department of Medicine, Northwestern University, Chicago, Illinois; [5]Retinal Circuits Development and Genetics Unit, National Eye Institute, Bethesda, Maryland; and [6]Faculty of Medicine, Research and Development Institute, Transilvania University of Brașov, Brașov, Romania

Abstract

Some previous studies in tissue fibrosis have suggested a profibrotic contribution from elevated expression of a protein termed either RGCC (regulator of cell cycle) or RGC-32 (response gene to complement 32 protein). Our analysis of public gene expression datasets, by contrast, revealed a consistent decrease in RGCC mRNA levels in association with pulmonary fibrosis. Consistent with this observation, we found that stimulating primary adult human lung fibroblasts with transforming growth factor (TGF)-β in cell cultures elevated collagen expression and simultaneously attenuated RGCC mRNA and protein levels. Moreover, overexpression of RGCC in cultured lung fibroblasts attenuated the stimulating effect of TGF-β on collagen levels. Similar to humans with pulmonary fibrosis, the levels of RGCC were also decreased *in vivo* in lung tissues of wild-type mice challenged with bleomycin in both acute and chronic models. Mice with constitutive RGCC gene deletion accumulated more collagen in their lungs in response to chronic bleomycin challenge than did wild-type mice. RNA-Seq analyses of lung fibroblasts revealed that RGCC overexpression alone had a modest transcriptomic effect, but in combination with TGF-β stimulation, induced notable transcriptomic changes that negated the effects of TGF-β, including on extracellular matrix-related genes. At the level of intracellular signaling, RGCC overexpression delayed early TGF-β–induced Smad2/3 phosphorylation, elevated the expression of total and phosphorylated antifibrotic mediator STAT1, and attenuated the expression of a profibrotic mediator STAT3. We conclude that RGCC plays a protective role in pulmonary fibrosis and that its decline permits collagen accumulation. Restoration of RGCC expression may have therapeutic potential in pulmonary fibrosis.

Keywords: response gene to complement 32 protein; regulator of cell cycle protein; lung fibrosis; idiopathic pulmonary fibrosis; scleroderma lung disease

Interstitial lung disease (ILD), and its defining component, pulmonary fibrosis, remain serious biomedical problems with no cure, limited therapeutic options, high morbidity, and rapid mortality. Excessive accumulation of scar tissue is particularly devastating in patients with idiopathic pulmonary fibrosis (IPF), systemic sclerosis (scleroderma)-associated ILD (SSc-ILD), and several other connective tissue diseases, including rheumatoid arthritis, poly- and dermatomyositis, and mixed connective tissue disease. A host of molecular mediators and processes drive fibrosis in ILD, and innovative therapeutic targeting of some of

(Received in original form January 14, 2021; accepted in final form October 20, 2021)

Supported by National Institutes of Health (NIH) grants NIAMS R01AR077562 and NHLBI R01HL126897, and VA Merit Award I01BX002499.

Author Contributions: I.G.L., V.R., H.R., and S.P.A. conceived of the study. I.G.L., B.S.H., A.V.M., and S.P.A. planned the experiments. I.G.L., V.L., B.S.H., R.F., and A.V.M. performed the experiments. N.W.T. provided human lung fibroblast tissues from patients and controls. I.G.L., V.L., and R.F. established and maintained primary fibroblast cultures from these tissues. V.R., T.C.B., and H.R. generated RGCC$^{-/-}$ mice and assisted with *in vivo* experiments. J.-P.C., B.S.H., and A.V.M. performed bioinformatics analyses. I.G.L. and S.P.A. analyzed and integrated the data and interpreted the findings, and all other authors contributed to data analyses and interpretations. I.G.L. and S.P.A. wrote the manuscript, and all authors contributed to manuscript editing and finalization.

Correspondence and requests for reprints should be addressed to Irina G. Luzina, M.D., Ph.D., Department of Medicine, University of Maryland School of Medicine, MSTF 834, 10 South Pine Street, Baltimore, MD 21201. E-mail: iluzina@som.umaryland.edu.

This article has a related editorial.

This article has a data supplement, which is accessible from this issue's table of contents online at www.atsjournals.org.

Am J Respir Cell Mol Biol Vol 66, Iss 2, pp 146–157, February 2022

Originally Published in Press as DOI: 10.1165/rcmb.2021-0022OC on October 20, 2021.
Internet address: www.atsjournals.org

them has already proven beneficial (1–3). Nevertheless, better therapies for ILD are much needed (2), and each newly identified molecular mediator represents a prospective therapeutic target.

RGCC (regulator of cell cycle), also known as RGC-32 (response gene to complement 32 protein), was recently described as a new profibrotic mediator in a different organ, the kidney (4–7). A recent report (8) similarly suggested that elevated RGCC may also contribute to early stages of bleomycin (BLM)-induced acute injury in mice. RGCC belongs to an ancient, although poorly characterized, superfamily of intracellular proteins that are present in all eukaryotes, including vertebrates, and contain the conserved sequence motif KLGDT (Figure 1A). Its two commonly used names, RGCC and RGC-32, underrepresent the breadth of its functional activities. Originally described and characterized by us (9, 10), this molecule is now known to contribute to the regulation of the cell cycle (5, 10, 11), cancer development (11–13), immune response (14–16), normal and abnormal angiogenesis (17–19), the biology of reproduction (19, 20), and metabolic control (21, 22). Guided by this combined evidence of RGCC's involvement in a spectrum of physiological and pathophysiological processes, including fibrosis (4–8), we set out to better define the role of RGCC in ILD. The findings presented below argue against the profibrotic role of elevated pulmonary RGCC and indicate that in the lungs, RGCC is a protective, antifibrotic mediator.

Methods

Primary Human Lung Fibroblast Cultures

Preexisting, already established through previous research, primary lung fibroblast cultures from deidentified adult human donors were used. The University of Maryland Institutional Review Board has made a "not human research" determination about these studies. Normal human lung fibroblast (NHLF) cultures from 9 distinct donors were sequentially numbered NHLF1–NHLF9, and lung fibroblast cultures from 6 patients with IPF were sequentially numbered IPF1–IPF6. Details of fibroblast culture and stimulation conditions are included in Supplementary Methods section.

Wild-Type and Genetically Manipulated Animals

Experiments were performed in wild-type (WT) female C57BL/6 mice aged 10–12 weeks (The Jackson Laboratory, Bar Harbor, Maine). Additionally, germline-deficient RGCC$^{-/-}$ (gene knockout, KO) mice were generated, bred, housed, and used as previously described (23). The animals were treated in accordance with a research protocol reviewed and approved by the University of Maryland Institutional Animal Care and Use Committee. Animals were maintained in sterile microisolator cages with sterile rodent feed and water. Daily maintenance of mice was performed at the Baltimore VA Medical Center Research Animal Facility and University of Maryland Animal Facility, which are approved by the Association for Assessment and Accreditation of Laboratory Animal Care. Acute and chronic bleomycin injuries were modeled as detailed in Supplementary Methods section.

RT-qPCR

Total RNA was isolated from lung tissues and fibroblast cultures using TRIzol (Thermo Fisher Scientific) and reversed-transcribed into cDNA using the SuperScript First-Strand synthesis kit from Invitrogen Life Technologies (Carlsbad, California). RT-qPCR was performed with SYBR Green PCR Master Mix (Life Technologies, Thermo Fisher Scientific) and validated primers for RGCC and COL1A2, which were obtained from Qiagen (Valencia, California). The levels of gene expression relative to 18S rRNA or GAPDH mRNA were calculated using the using the $2^{-\Delta\Delta Ct}$ method.

Western Blotting

Western blotting was performed using the Novex (ThermoFisher) system per the manufacturer's recommendations. All PVDF membranes were blocked and incubated with primary and secondary antibodies using Tris-buffered saline with 0.1% Tween 20 and 5% bovine serum albumin. Specific antibodies used for Western blotting are listed in the Supplementary Methods section. Membranes were developed using SuperSignal West Pico Chemiluminescent Substrate (Thermo Scientific).

Measurement of Total Lung Collagen

Total lung collagen was measured based on the quantification of hydroxyproline, using the colorimetric QuickZyme assay (QuickZyme BioSciences, Leiden, the Netherlands), according to the manufacturer's recommendations, as described. Briefly, following hydrolysis of 50 mg of lung tissue in 500 μl of 6M HCl for 20 hours at 95°C, the hydrolysate was diluted 10-fold with 4M HCl and measured against serial dilutions of collagen standard. The results were expressed as μg collagen per mg wet lung tissue.

RNA-Seq

RNA-sequencing analysis of differentially treated NHLF was performed by Otogenetics Corporation (Atlanta, Georgia). Detailed RNA-Seq procedures and analyses are included in the Supplementary Methods section. The RNA-Seq data have been deposited in the NCBI GEO database (accession number GSE158542).

Statistical Analyses

Experimental data were expressed as mean ± S.D. values. Differences between sample groups were calculated using a two-tailed Student's *t* test or a Mann-Whitney *U* test.

Results

The Expression Levels of RGCC Are Decreased in Humans and Mice with Pulmonary Fibrosis

Analysis of our recently reported RNA-Seq dataset (24) revealed decreased RGCC mRNA levels in the scarred IPF lung tissues compared with healthy control and normal-appearing IPF tissues (Figure 1B). RT-qPCR analyses for RGCC mRNA in a different set of lung tissue samples similarly revealed that the levels of RGCC mRNA were consistently lower in the lungs of patients with IPF or SSc-ILD compared with healthy controls (Figure 1C). Analyses of our single-cell RNA-Seq dataset (25) for RGCC mRNA expression uncovered that in the lungs, type 1 alveolar epithelial cells, ciliated epithelial cells, fibroblasts, and macrophages expressed notable levels of this mRNA (Figure 1D). Comparative assessment of RGCC expression in pulmonary cell types of patients and controls suggested lower levels in several cell types, most notably in lung fibroblasts from fibrotic lungs (Figure 1E). Subset analyses focused on pulmonary fibroblasts unveiled that indeed, these cells expressed RGCC at higher levels in healthy controls than in ILD patients (Figure 1F). Western blotting of lung tissue homogenates

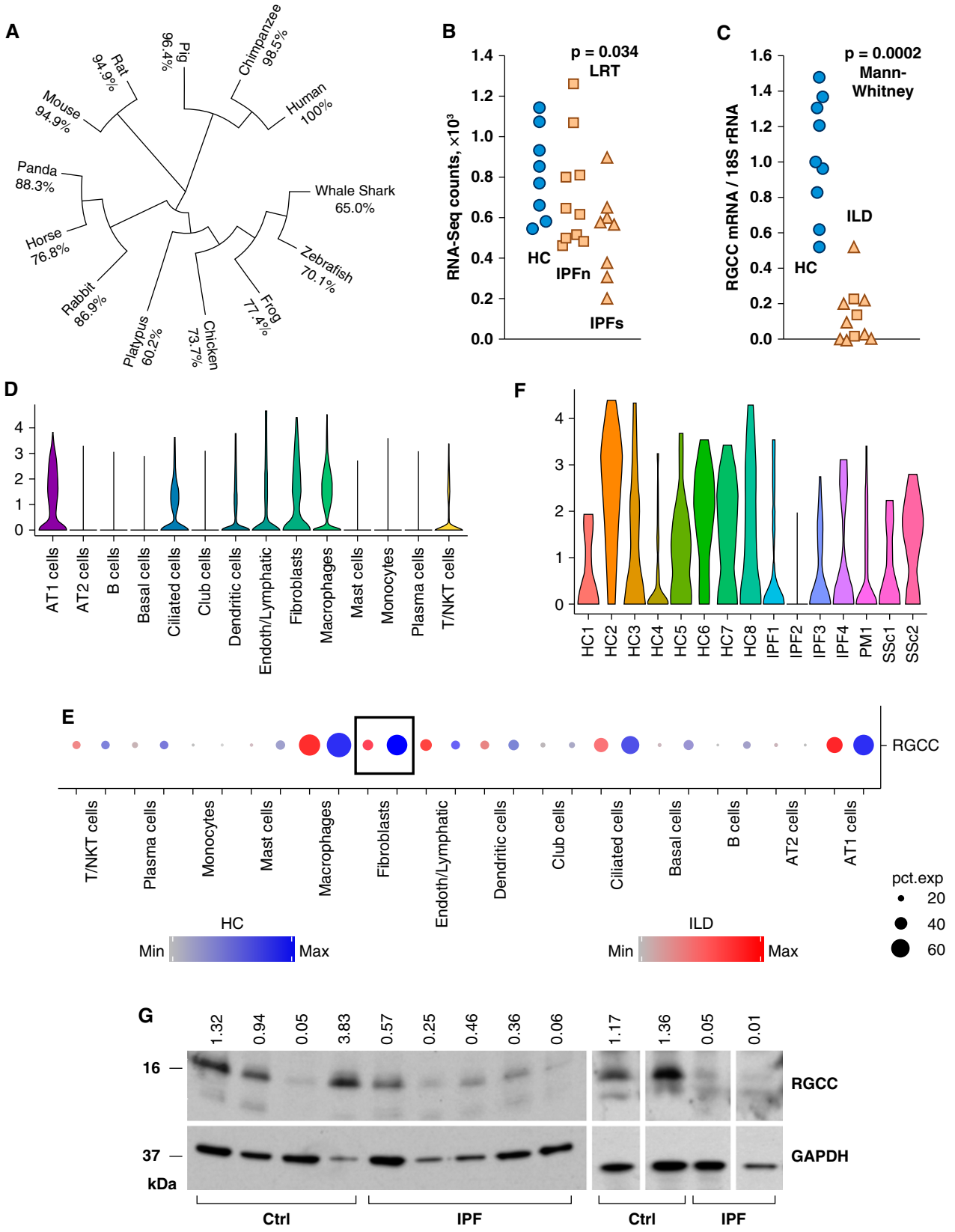

Figure 1. Expression levels of RGCC (regulator of cell cycle) in the lungs of patients with interstitial lung disease (ILD) and healthy controls. (*A*) Phylogenetic tree of RGCC proteins by species. Percent similarities with human RGCC are indicated. (*B*) Normalized DESeq2 counts from bulk RNA-Seq of lung samples from macroscopically normal-appearing and scarred areas of with idiopathic pulmonary fibrosis (IPF) lungs (IPFn

from patients with IPF confirmed lower RGCC protein expression levels than in healthy donors (Figure 1G). The difference in normalized RGCC band densities between patients and controls was significant by Mann-Whitney *U* test ($P = 0.032$) or close to significant by two-tailed Student's *t* test ($P = 0.069$). Others also found that RGCC is pronouncedly expressed in a cell subset denoted as pulmonary lipofibroblasts and that lipofibroblasts from healthy controls express significantly more RGCC than such cells from the lungs of patients with IPF (26). It appears that RGCC is decreased, not elevated, in the lungs of patients with ILD, particularly, IPF.

Prompted by this inconsistency with previous reports suggesting a profibrotic role for RGCC (4, 6–8), we analyzed RGCC mRNA expression levels in the lungs of bleomycin-challenged mice utilizing publicly available gene series expression data GSE131800 from the National Center for Biotechnology Information Gene Expression Omnibus (GEO), as reported in (27). The expression levels of RGCC mRNA were lower in pulmonary epithelial cells, fibroblasts, and macrophages of bleomycin-challenged mice (*see* online supplement, Figure E1). Additional searches of other existing relevant GEO datasets were performed for changes in RGCC mRNA levels, revealing lower RGCC mRNA levels in fibrotic lung tissues as well as attenuation of RGCC mRNA expression by stimulation with TGF-β in various cultured cell types (Table E1).

Guided by this combined evidence of decreased RGCC expression in human and mouse tissues and cells in relation to pulmonary fibrosis, we hypothesized that RGCC protects against pulmonary fibrosis, thus challenging the established notion of its profibrotic role (4–8).

TGF-β Suppresses the Expression of RGCC in Cultured Lung Fibroblasts

Experiments were performed to determine whether the difference in RGCC expression between NHLFs and IPF lung fibroblasts persists in cell culture. While IPF lung fibroblasts consistently maintained their fibrotic phenotype in culture based on elevated production of collagen and α-SMA, the differences in basal RGCC expression between IPF fibroblasts and NHLFs were not consistently maintained, with apparent heterogeneity in RGCC expression levels in each of the groups of cell cultures (Figure 2A). This observation suggested that the decrease in RGCC levels observed in the lung tissues (Figure 1) was not intrinsic to the origin of the cells but was induced by aspects of the pulmonary milieu *in vivo*, which were lost with culture passaging. Consistent with this notion, NHLFs and IPF lung fibroblasts similarly responded to stimulation with rhTGF-β in culture by decreasing the levels of RGCC mRNA while increasing the levels of collagen mRNA (Figure 2B) and by decreasing the levels of RGCC protein (Figure 2C, $P = 0.013$, two-tailed paired *t* test across all samples).

To determine whether the observed lower RGCC levels in patients (Figure 1) and in cell culture (Figures 2B and 2C) might play a mechanistic role, the effect of plasmid-mediated overexpression of RGCC in cultured fibroblasts was assessed. RGCC overexpression strongly attenuated the magnitude of the increase in collagen in response to TGF-β stimulation in both primary NHLFs and IPF-derived fibroblasts (Figure 2D). Similar findings were made in a separate experiment with NHLF9 and IPF5.

Low RGCC Expression Is Associated with and Contributes to Pulmonary Fibrosis in Mice

Consistent with the findings in human lung tissues and fibroblast cultures (Figures 1 and 2), pronounced declines in the levels of RGCC mRNA (Figure 3A) and protein (Figure 3B) were observed following acute bleomycin injury to the lungs. However, $RGCC^{-/-}$ mice accumulated less collagen in their lungs post-intratracheal bleomycin challenge than did their WT control counterparts (Figure 3C). This finding is consistent with a similar recent observation of others (8), but it contradicts the notions developed above regarding the possible associative and causative links between lower RGCC and higher collagen levels in pulmonary fibrosis. To explore this contradiction, we considered that the acute bleomycin injury model does not fully represent the chronic nature of human pulmonary fibroses. A chronic bleomycin model was studied in $RGCC^{-/-}$ and WT mice, in which mice received bleomycin intraperitoneally twice a week for four weeks with analyses performed on day 33. The levels of RGCC were pronouncedly lowered in chronically bleomycin-challenged mice (Figure 3B). Fibroblasts outgrown from the lungs of chronically bleomycin-challenged mice retained their low RGCC-expressing phenotype in cell culture after repetitive passaging (Figure E2). RGCC deficiency did not affect the dynamics of total body weight in neither saline nor bleomycin-treated mice in the chronic bleomycin model (Figure 3D). Histologically, central areas of the lungs were spared, whereas peripheral focal pleural thickening and subpleural peripheral deposition of collagen combined with mild cellular infiltrates were similarly observed in $RGCC^{-/-}$ as well as WT mice (Figure 3E). Total and differential bronchoalveolar lavage cell counts were similarly affected by the chronic bleomycin exposure in both $RGCC^{-/-}$ and WT groups of mice (Figure 3F). Nevertheless, consistent with the findings in humans (Figures 1 and 2) and distinct from the findings in the acute bleomycin model (Figure 3C), $RGCC^{-/-}$ mice chronically challenged with bleomycin accumulated more collagen than their WT counterparts (Figure 3G). Thus, like humans, RGCC deficiency is permissive of lung fibrosis in mice in the chronic bleomycin model, which reproduces the features of human pulmonary fibrosis more accurately than does the acute intratracheal model.

Figure 1. (*Continued*). and IPFs, respectively) as well as from HC (24). The indicated *P* value was calculated using the DESeq2 likelihood ratio tests. (*C*) RT-qPCR for RGCC mRNA normalized to 18S rRNA levels and further normalized to the average of the control group; in the ILD group, tissue samples from patients with IPF are denoted with triangles whereas the SSc-ILD tissue samples are denoted with squares. The indicated *P* value was calculated using Mann-Whitney *U* test. (*D*) Violin plot of RGCC expression in pulmonary cell population clusters (25). (*E*) Split dot-plots of RGCC expression in the indicated pulmonary cell types. Blue dots denote HC, whereas red dots indicate patients with ILD described in (25). (*F*) Violin plots of RGCC expression in the fibroblast cluster control and ILD lungs (25). (*G*) Western blotting for RGCC in lung homogenates obtained from healthy controls (Ctrl) and patients with IPF. The ratios of RGCC band densities to their corresponding GAPDH bands are indicated above the gels. AT1 = alveolar type 1; HC = healthy controls; IPF = idiopathic pulmonary fibrosis; Max = maximum; Min = minimum; NKT = natural killer T; PM = polymyositis; SSc = systemic sclerosis.

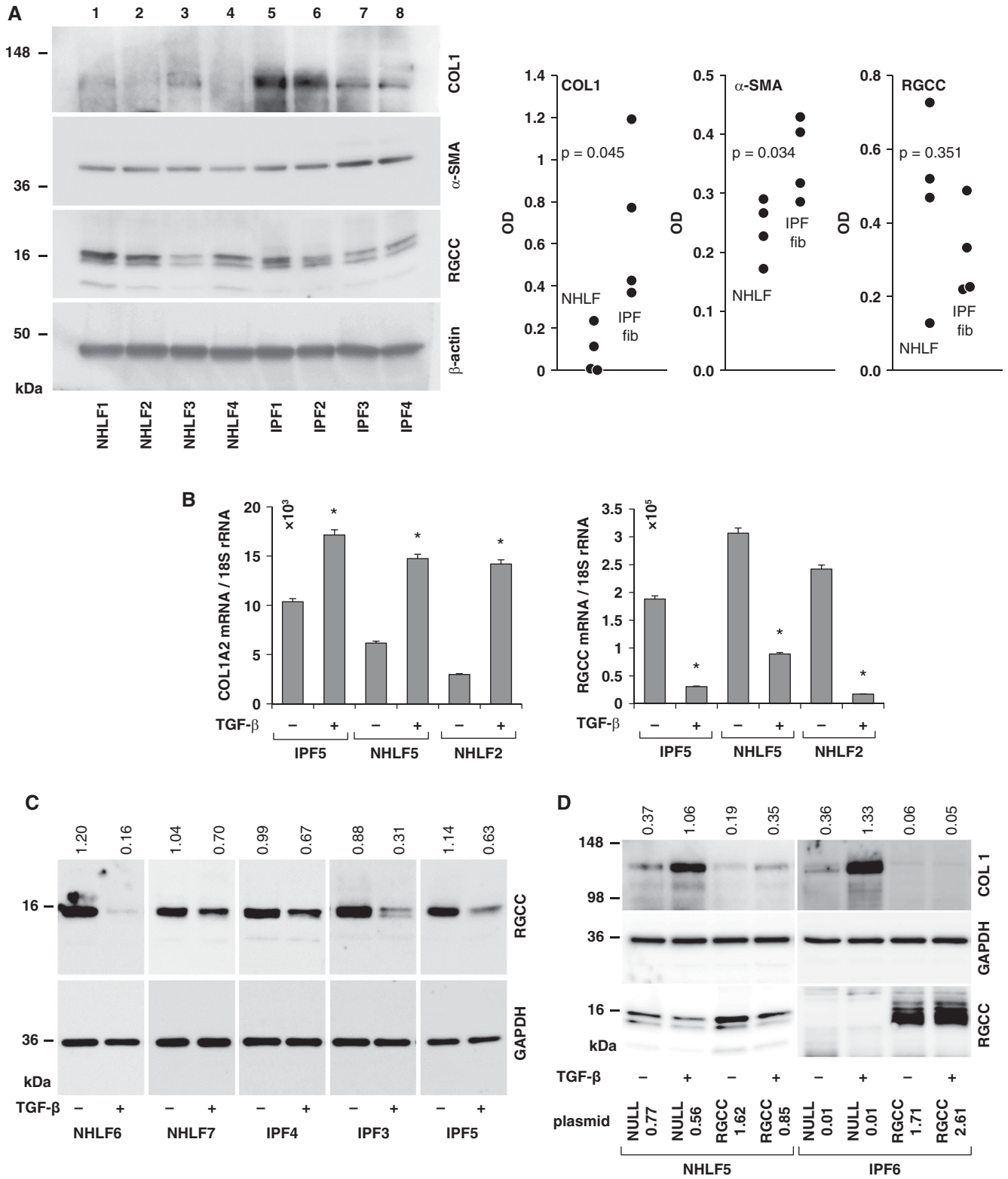

Figure 2. RGCC expression in primary lung fibroblast cultures. (*A*) Western blotting of primary fibroblast lysates for COL1, α-SMA, RGCC, and β-actin. The ratios of COL1, α-SMA, and RGCC band densities to their corresponding β-actin bands as well as statistical significance of differences between normal human lung fibroblast (NHLF) and IPF fibroblasts are shown in the scatterplots on the right. (*B*) RT-qPCR for collagen I (α2) and RGCC mRNA in NHLFs and IPF lung fibroblast cultures that were or were not stimulated with 5 ng/ml of TGF-β. Asterisk indicates significant differences (*$P < 0.05$) in triplicate TGF-β–stimulated versus control cultures for each condition. (*C*) Western blotting of

Transcriptomic Effects of RGCC Overexpression in Cultured Lung Fibroblasts

To begin addressing possible mechanistic reasons for the observed antifibrotic effect of elevated RGCC expression, transcriptomic effects of RGCC overexpression in NHLF were assessed, alone and in combination with TGF-β–mediated activation. Primary lung fibroblast cultures from two separate donors (NHLF6 and NHLF8) were each transfected with the RGCC-encoding or the noncoding control (NULL) plasmids, and, after 24 hours, stimulated with rhTGF-β or PBS. After an additional 24 hours, cells were harvested, and their transcriptomes analyzed by RNA-Seq. Thus, four groups of differentially activated cells were compared (Figure E3), with two separate cell cultures per group: NULL, NULL+TGF-β, RGCC, RGCC+TGF-β. Pairwise comparisons of transcriptomes between these groups are shown in Figure 4A. Perhaps not surprisingly, stimulation with TGF-β affected the expression levels of numerous genes (Figure 4A, left). Interestingly, the numbers of upregulated and downregulated genes were less affected by RGCC overexpression alone (Figure 4A, middle). Yet, in combination with TGF-β stimulation, RGCC overexpression had a greater impact on the numbers of affected genes (Figure 4A, right). Genes with the greatest magnitude of modulation in these comparisons are listed in Tables E2–E5. These data indicate that the transcriptomic effect of elevated RGCC expression alone is relatively modest, whereas the modulating effect of elevated RGCC on TGF-β–induced changes are pronounced.

Further analyses of these transcriptomic data were performed utilizing Metascape (28). The lists of up- and downregulated genes identified by DESeq2 analyses in the indicated pair-wise comparisons were analyzed for functional gene enrichment (Figure 4B), revealing a broad spectrum of transcriptomic effects of RGCC overexpression on diverse pathways and processes. The breadth of such regulation awaits further exploration. In relevance to fibrosis, extracellular matrix organization and morphogenesis were among the top enriched pathways and processes (Figure 4B). Of note, top enriched terms from the list of genes elevated by TGF-β treatment (NULL+TGF-β versus NULL elevated) clustered with the enriched terms from the list of genes attenuated by RGCC overexpression in TGF-β–treated cells (RGCC+TGF-β versus NULL+TGF-β decreased). Reciprocally, top enriched terms from the list of genes whose expression was attenuated by TGF-β treatment (NULL+TGF-β versus NULL decreased) clustered with the enriched terms from the list of genes elevated by RGCC overexpression in TGF-β–treated cells (RGCC+TGF-β versus NULL+TGF-β elevated). These findings indicate that elevated RGCC expression broadly negates the effects of TGF-β stimulation on NHLFs. Such converse transcriptomic regulation of the TGF-β effects by elevated RGCC is further illustrated by the Metascape-generated Circos plot (Figure 4C). A more detailed analysis of extracellular matrix-related genes whose expression was elevated by TGF-β stimulation and then attenuated by elevated RGCC is shown in Figure 4D.

Signaling Pathways Affected by Elevated RGCC Expression

To follow up on the observed interaction between elevated RGCC and stimulation with TGF-β, experiments were performed to assess the effect of RGCC overexpression on Smad2/3 phosphorylation (Figure 5A). RGCC overexpression attenuated early Smad2/3 phosphorylation response to TGF-β stimulation at 15 min in NHLF1. Similar findings were made in NHLF4. We then considered known positive and negative regulators of TGF-β signaling by revisiting the RNA-Seq results (Figure 4) for possible changes in the expression of such regulators. These analyses revealed that RGCC overexpression did not affect, either by itself or in combination with TGF-β stimulation, the expression levels of TGFB1, TGFB2, TGFB3, TGFBR1, TGFBR2, SMAD1, SMAD2, SMAD3, SMAD4, SMAD7, JAK1, JAK3, STAT1, STAT3, STAT6, AP2B1, BAMBI, NEDDL4, SMURF2, RNF111 (Arkadia), EP300, SKI, or SKIL (SnoN) genes. It was possible that expression of some of these regulators was affected by RGCC at the post-transcriptional level. To address this possibility, Western blotting analyses of NULL-transfected or RGCC-overexpressing NHLFs and IPF-derived fibroblasts were performed for negative regulators of TGF-β signaling, Ski and SnoN (Figure E4), revealing that RGCC overexpression did not elevate but suppressed the levels of Ski, indicating that it is an unlikely inhibitory mediator of the antifibrotic action of RGCC. The expression of SnoN was minimal, with or without RGCC overexpression. In similar experiments, striking observations were made regarding an important antifibrotic mediator, STAT1 (29–31), the levels of which were elevated by RGCC overexpression, and which was present in its phosphorylated form (Figure 5B). At the same time, the levels of JAK1, which is upstream of STAT1 in the signaling cascade, as well as the levels of another known regulator of fibrosis, STAT3 (32–34), were decreased (Figure 5B).

Discussion

The presented data indicate that RGCC expression levels are decreased in pulmonary fibrosis in humans (Figure 1, Table E1) as well as in mice challenged with bleomycin, either acutely or chronically (Figures 3A and B; Figure E1). Consistent with these observations and the established notion of profibrotic regulation by TGF-β, cultured primary lung fibroblasts responded to stimulation with TGF-β by decreasing the expression levels of RGCC mRNA (Figure 2B, Table E1) and protein (Figure 2C). These combined observations raised an important question as to whether the observed decline in RGCC levels contributed to the development of fibrosis mechanistically or, alternatively, was an independent fibrosis-associated effect with no causative mechanistic contribution. In cell culture, overexpression of RGCC attenuated TGF-β–stimulated increase in collagen (Figure 2D), whereas gene deletion of RGCC in mice *in vivo* aggravated bleomycin-

Figure 2. (*Continued*). primary fibroblast lysates for RGCC and GAPDH. NHLF and IPF lung fibroblast cultures were or were not stimulated with 5 ng/ml of TGF-β. The ratios of RGCC band densities to their corresponding GAPDH bands are indicated above the gel. (*D*) Effect of plasmid-based RGCC gene delivery to NHLFs and IPF lung fibroblasts on TGF-β–activated type I collagen protein expression. Western blots for type I collagen, GAPDH, and RGCC are shown. The ratios of collagen band densities to their corresponding GAPDH bands are indicated above the gels, and the ratios of RGCC bands to GAPDH are shown next to the indications of the plasmids used for cell transfections below the gels. α-SMA = α-smooth muscle actin; COL1 = collagen type 1; OD = optical density; TGF = transforming growth factor.

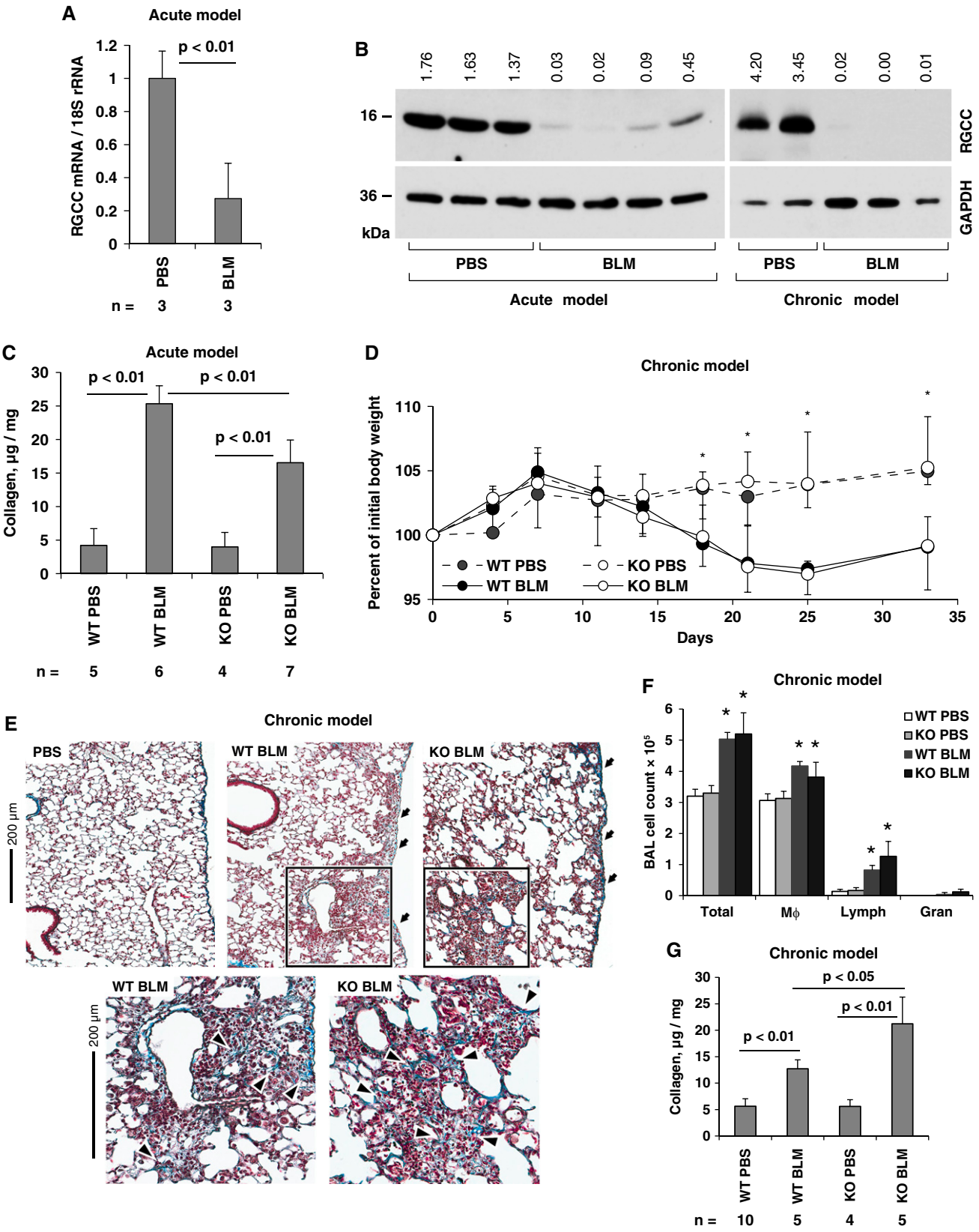

Figure 3. Pulmonary changes induced in WT and RGCC KO mice by acute or chronic bleomycin (BLM) challenges in comparison to similarly challenged with PBS control animals. (*A*) RT-qPCR results for RGCC mRNA in the acute bleomycin injury model. (*B*) Western blotting for RGCC and GAPDH in lung homogenates obtained from bleomycin-challenged mice in the acute and chronic bleomycin injury models. (*C*) Total lung collagen, microgram per milligram of wet lung tissue, after acute bleomycin challenge. (*D*) Time-dependent changes in total body weight of

induced fibrosis in the chronic exposure model (Figure 3G). These observations are indicative of not only the associative link between low RGCC and fibrosis but also of a mechanistic participation of RGCC in the regulation of the fibrotic process.

The internal consistency of this overall dataset was challenged by the protective antifibrotic, instead of augmenting profibrotic, effect RGCC gene depletion in the acute bleomycin injury model (Figure 3C). Others (8) made a similar observation in this model. The inconsistency is likely due to the inflammation-dependent nature of the acute bleomycin injury, which models the substantially less inflammation-dependent chronic pulmonary fibroses in humans less accurately than does the chronic bleomycin model (35–42). The chronic bleomycin model is also similar to human pulmonary fibroses in its histopathological appearance with geographically heterogenous, patchy involvement, which is distributed mostly peripherally, sparing the central regions of the lungs. In the chronic bleomycin model, RGCC deficiency had no effect on the dynamics of the total body weight (Figure 3D), pulmonary histopathology (Figure 3E), or accumulation of inflammatory cells (Figure 3F), indicating that RGCC deficiency does not regulate the mild chronic lung inflammation in this model. Yet, RGCC deficiency permitted a more pronounced deposition of collagen in the lungs of chronically bleomycin-challenged mice (Figure 3G), making it a regulator of fibrosis, but not inflammation, in the chronic profibrotic injury relevant to human disease. By contrast, RGCC deficiency protects from the acute inflammation-driven fibrosis by interacting with fibrosis-propelling immune mechanisms (8). Similar considerations may explain the disconnect between our findings and the previously reported observations in kidney fibrosis (4–7), which implicated elevated and not decreased levels of RGCC in the disease pathogenesis. It is also possible that pro- and antifibrotic regulation by RGCC might depend on the affected cell type (epithelial and endothelial cells, fibrocytes, pericytes, macrophages, and lymphocytes), which, in combination with natural differences and renal and pulmonary cellularity and physiology, may explain organ- and tissue-dependent regulation of fibrosis by RGCC.

To begin addressing possible molecular pathways that are involved in the direct antifibrotic regulation by RGCC, RNA-Seq analyses of transcriptomic changes were performed (Figure 4). Plasmid-mediated overexpression of RGCC alone affected the expression of fewer genes than did stimulation of NHLFs with rhTGF-β (Figure 4A). However, overexpression of RGCC resulted in much more pronounced effects on TGF-β–stimulated NHLFs based on the counts of up- and downregulated genes (Figure 4A). We observed, for the first time to our knowledge, that RGCC overexpression affected the expression levels of the genes in several biomedically central and functionally diverse pathways and processes, as demonstrated by the gene ontology enrichment analysis (Figure 4B). The breadth and impact of such complex regulation remains to be explored. In relevance to tissue fibrosis, extracellular matrix organization and tissue morphogenesis were among the top enriched pathways and processes (Figure 4B). Particularly relevant, genes with the expression levels attenuated by RGCC in TGF-β–stimulated cells were similar to those upregulated by TGF-β stimulation alone based on enrichment clustering, whereas genes elevated by RGCC overexpression in TGF-β–stimulated cells were similar to those downregulated by TGF-β stimulation alone (Figures 4B and C). Among connective tissue-related genes regulated in such a fashion were genes for collagen chains, elastin, lysyl oxidase-like 3, prolyl 3-hydroxylases and other genes listed in Figure 4D. These transcriptomic observations further support the notion of antifibrotic regulation by RGCC. The intrinsic fibroblastic mechanisms through which RGCC exerts its antifibrotic effect remain to be elucidated.

At the level of intracellular signaling, RGCC overexpression delayed TGF-β–induced Smad2/3 phosphorylation (Figure 5A), as well as affected the expression levels of STAT1, JAK1, and STAT3 (Figure 5B). Negative regulators of TGF-β signaling, Ski and SnoN, were unlikely mediators of the antifibrotic regulation by RGCC (Figure E4). The findings in Figure 5B are interesting for several reasons. First, the RNA-Seq analyses did not suggest an RGCC-driven change in the expression of mRNAs for STAT1, JAK1, or STAT3, yet these proteins were affected by elevated RGCC. The complexity of not only transcriptomic (Figure 4) but also post-transcriptional proteomic regulation by RGCC need to be explored in future studies. Second, although not only the total but also phosphorylated STAT1 were elevated, the expression of JAK1 was attenuated in the presence of RGCC, raising the question about the upstream mediator of STAT1 phosphorylation. This mechanistic question also needs to be answered in the future. Third, the RGCC-driven elevated expression of total and phosphorylated STAT1, although occurring for mechanistic reasons that are yet to be understood, has far-reaching consequences. STAT1 is the central mediator of intracellular signaling from receptors for interferons, IL-27, IL-35, and IL-39 (29–31). STAT1-mediated regulation of fibrosis is complex (43–46), with such complexity driven by several factors. In addition to signaling from numerous, functionally diverse receptors, it also differentially regulates diverse cell types that are involved in the fibrotic process. Such differential regulation specifically contributes to the intricate interplay between, on the one hand, acute and chronic inflammation, and on the other hand, the fibrotic process, which often co-occur in response to injuries. Furthermore, the immediate and long-term effects of altered STAT1 activity may be different.

Figure 3. (*Continued*). mice in the chronic bleomycin model. Asterisk indicates significant differences (*$P < 0.05$) between BLM-treated and PBS-treated mice. (*E*) Trichrome staining of lung sections from mice in the chronic bleomycin model imaged at lower (top row) and higher (bottom row) magnifications. The framed areas of the lower-magnification images are shown at a higher magnification in the bottom row. Scale bars (left side of each row), 200 μm. Selected areas of plural thickening are indicated with arrows, and collagen fibers appearing in blue are indicated with arrowheads. (*F*) Total and differential cell counts in bronchoalveolar lavage samples from mouse lungs in the chronic bleomycin model. Asterisk indicates significant increases (*$P < 0.05$) in bleomycin-challenged animals compared with PBS controls. (*G*) Total lung collagen, microgram per milligram of wet lung tissue, after chronic bleomycin challenge. In *A*, *C*, and *G*, the numbers of animals tested in each group (*n*) are shown, as well as *P* values calculated using a two-tailed Student's *t* test for the indicated pairwise comparisons. In *D*, *E*, and *F*, data represent 4–5 animals tested for each experimental condition. Gran = granulocytes; KO = knockout; Lymph = lymphocytes; MΦ = macrophages; WT = wild-type.

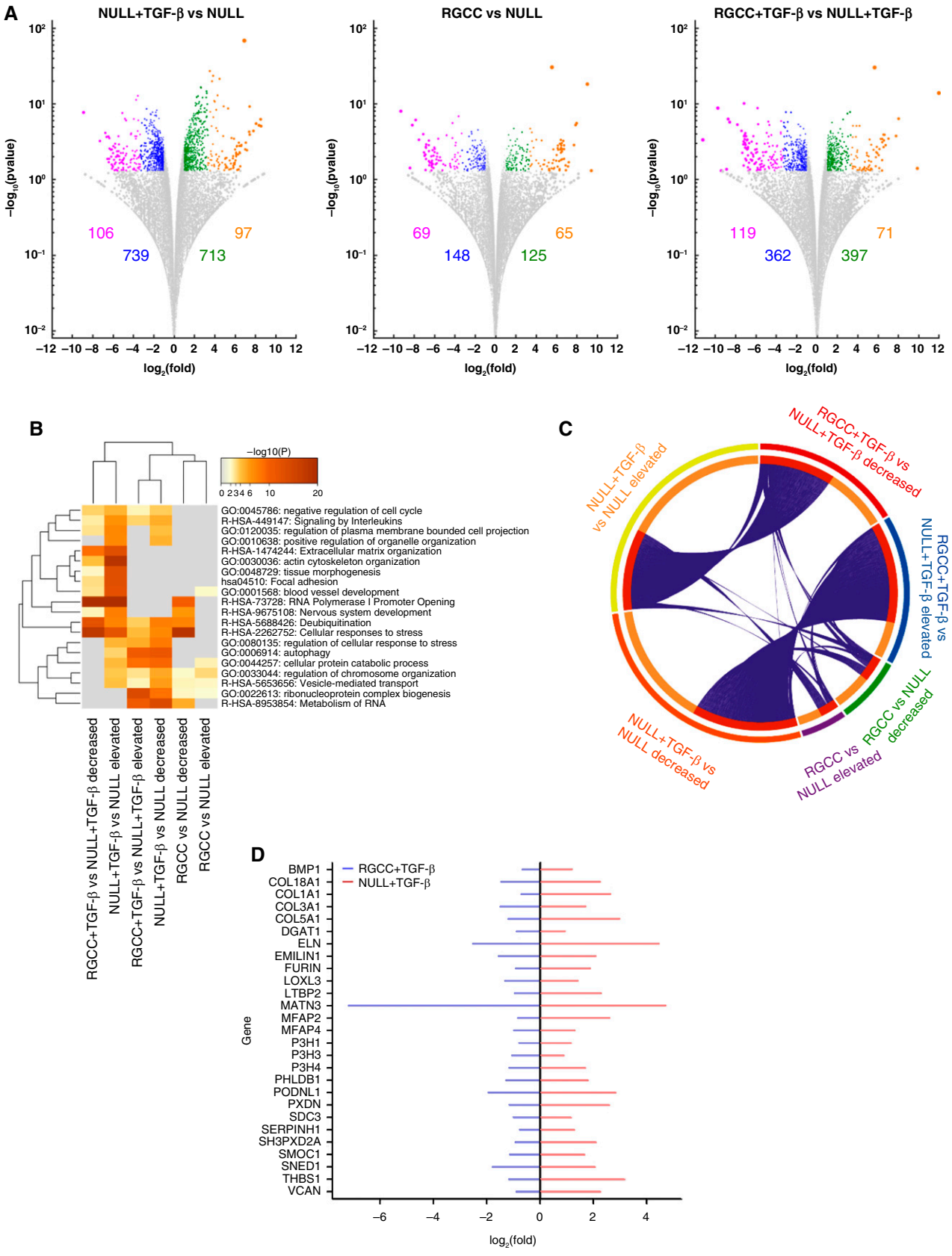

Figure 4. Transcriptomic effects of RGCC overexpression in NHLFs. (*A*) Volcano plots [$-\log_{10}$(*P* value) versus $\log_2$(fold)] of genes in the indicated comparisons. Selection criteria for up- and downregulated genes included significant differences ($P < 0.05$) as well as fold-difference

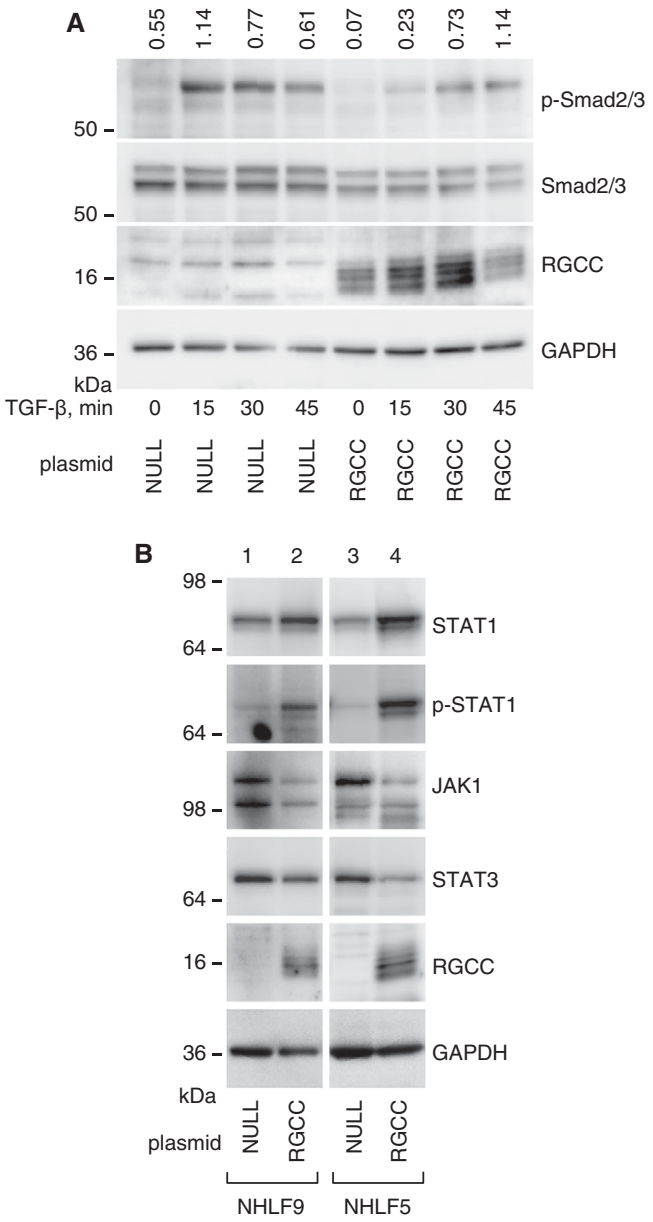

Figure 5. Effect of RGCC overexpression on selected intracellular signaling mediators. (*A*) Smad2/3 phosphorylation, after stimulation with rhTGF-β for indicated times, in NHLF1 transfected with either noncoding NULL or RGCC-encoding plasmids. The ratios of phosphorylated to total Smad2/3 densities are indicated above the corresponding Western blotting gel lanes. (*B*) Western blotting for indicated intracellular signaling mediators in NHLF transfected with the RGCC-encoding or control NULL plasmids.

Nevertheless, STAT1 deficiency is generally profibrotic (43–46), whereas elevated STAT1 expression and activation are antifibrotic (47, 48) including, in consistency with Figure 5A, inhibition of TGF-β signaling through the Smad pathway (47).

Our findings not only demonstrate the protective role of RGCC in pulmonary fibrosis but also lay the ground for future mechanistic and translational work. In addition to the already mentioned need to understand the molecular mechanisms and specific functional consequences of transriptomic and proteomic regulation by RGCC, many other questions remain to be answered. Is RGCC similarly protective against fibrosis in other organs and tissues? Does RGCC, a reported interactor with cell cycle proteins, regulate cell proliferation and survival in relevance to fibrosis? Does RGCC, a known regulator of epithelial–mesenchymal transition (EMT) in renal tubular cells (4, 5) and in cancers (7, 49, 50), regulates EMT in the lungs in relevance to ILD? More broadly, what are the pathophysiological consequences of decreased RGCC in cell types other than fibroblasts, e.g., epithelial cells or macrophages, and what is the therapeutic potential of broad versus cell-type-specific restoration of RGCC expression? These topics will be interrogated in future studies.

In conclusion, this report links, for the first time, attenuated—not elevated—RGCC/RGC-32 expression with a serious malady, pulmonary fibrosis. More specifically, human pulmonary fibrosis and chronic bleomycin model of pulmonary fibrosis are associated with and likely driven by lowered expression levels of RGCC/RGC-32. Overexpression of RGCC in primary fibroblasts elicits broad, including antifibrotic, transcriptomic effects; delays TGF-β–induced Smad2/3 phosphorylation; induces the levels of total and phosphorylated antifibrotic signaling

Figure 4. (*Continued*). between groups. The total numbers of genes meeting the selection criteria for elevated (orange for > 10-fold increase and green for 2–10-fold increase) or reduced (purple for > 10-fold decrease and blue for 2–10-fold decrease) expression are indicated in each panel. (*B*) Pathway and process enrichment analyses of differentially expressed genes were performed in Metascape. Clustering of the resulting top enriched terms and of the indicated pairwise comparisons is represented as the heatmap. The colors denote the negative $\log_{10}$ of *P* values for pathway/process enrichment. (*C*) Metascape-generated Circos visualization of overlaps among gene lists corresponding to indicated pairwise comparisons. Gene pairs falling into the same enrichment term linkage are represented with blue curves. (*D*) Changes in the expression levels of selected indicated extracellular matrix-related genes induced by TGF-β stimulation (red) or RGCC overexpression in TGF-β–stimulated cells (blue). The elevated expression in response to stimulation with TGF-β is indicated as $\log_2$ fold difference from NULL-transfected cells without additional stimulation. The downregulated gene expression in RGCC-overexpressing cells is shown as $\log_2$ fold difference from NULL-transfected and additionally TGF-β–treated cells.

mediator, STAT1; attenuates the levels of a profibrotic mediator, STAT3; and attenuates TGF-β–induced collagen levels. It is possible that restoration of RGCC/RGC-32 expression levels may be therapeutic in pulmonary fibrosis. The mechanistic basis of RGCC/RGC-32 depletion-driven pulmonary fibrosis needs to be better understood, and the therapeutic potential of restoration of the expression of RGCC/RGC-32 needs to be explored. ■

Author disclosures are available with the text of this article at www.atsjournals.org.

References

1. Lederer DJ, Martinez FJ. Idiopathic pulmonary fibrosis. *N Engl J Med* 2018;378:1811–1823.
2. Dempsey TM, Payne S, Sangaralingham L, Yao X, Shah ND, Limper AH. Adoption of the antifibrotic medications pirfenidone and nintedanib for patients with idiopathic pulmonary fibrosis. *Ann Am Thorac Soc* 2021;18: 1121–1128.
3. Di Martino E, Provenzani A, Vitulo P, Polidori P. Systematic review and meta-analysis of pirfenidone, nintedanib, and pamrevlumab for the treatment of idiopathic pulmonary fibrosis. *Ann Pharmacother* 2021;55: 723–731.
4. Guo X, Jose PA, Chen SY. Response gene to complement 32 interacts with Smad3 to promote epithelial-mesenchymal transition of human renal tubular cells. *Am J Physiol Cell Physiol* 2011;300:C1415–C1421.
5. Shen YL, Liu HJ, Sun L, Niu XL, Kuang XY, Wang P, *et al.* Response gene to complement 32 regulates the G2/M phase checkpoint during renal tubular epithelial cell repair. *Cell Mol Biol Lett* 2016;21:19.
6. Li Z, Xie WB, Escano CS, Asico LD, Xie Q, Jose PA, *et al.* Response gene to complement 32 is essential for fibroblast activation in renal fibrosis. *J Biol Chem* 2011;286:41323–41330.
7. Wang XY, Li SN, Zhu HF, Hu ZY, Zhong Y, Gu CS, *et al.* RGC32 induces epithelial-mesenchymal transition by activating the Smad/Sip1 signaling pathway in CRC. *Sci Rep* 2017;7:46078.
8. Sun C, Chen SY. RGC32 promotes bleomycin-induced systemic sclerosis in a murine disease model by modulating classically activated macrophage function. *J Immunol* 2018;200:2777–2785.
9. Badea TC, Niculescu FI, Soane L, Shin ML, Rus H. Molecular cloning and characterization of RGC-32, a novel gene induced by complement activation in oligodendrocytes. *J Biol Chem* 1998;273:26977–26981.
10. Badea T, Niculescu F, Soane L, Fosbrink M, Sorana H, Rus V, *et al.* RGC-32 increases p34CDC2 kinase activity and entry of aortic smooth muscle cells into S-phase. *J Biol Chem* 2002;277:502–508.
11. Saigusa K, Imoto I, Tanikawa C, Aoyagi M, Ohno K, Nakamura Y, *et al.* RGC32, a novel p53-inducible gene, is located on centrosomes during mitosis and results in G2/M arrest. *Oncogene* 2007;26:1110–1121.
12. Lu Y, Hu XB. C5a stimulates the proliferation of breast cancer cells via Akt-dependent RGC-32 gene activation. *Oncol Rep* 2014;32: 2817–2823.
13. Kim DS, Lee JY, Lee SM, Choi JE, Cho S, Park JY. Promoter methylation of the RGC32 gene in nonsmall cell lung cancer. *Cancer* 2011;117:590–596.
14. Tang R, Zhang G, Chen SY. Response gene to complement 32 protein promotes macrophage phagocytosis via activation of protein kinase C pathway. *J Biol Chem* 2014;289:22715–22722.
15. Zhao P, Gao D, Wang Q, Song B, Shao Q, Sun J, *et al.* Response gene to complement 32 (RGC-32) expression on M2-polarized and tumor-associated macrophages is M-CSF-dependent and enhanced by tumor-derived IL-4. *Cell Mol Immunol* 2015;12:692–699.
16. Rus V, Nguyen V, Tatomir A, Lees JR, Mekala AP, Boodhoo D, *et al.* RGC-32 promotes Th17 cell differentiation and enhances experimental autoimmune encephalomyelitis. *J Immunol* 2017;198:3869–3877.
17. An X, Jin Y, Guo H, Foo SY, Cully BL, Wu J, *et al.* Response gene to complement 32, a novel hypoxia-regulated angiogenic inhibitor. *Circulation* 2009;120:617–627.
18. Wang JN, Shi N, Xie WB, Guo X, Chen SY. Response gene to complement 32 promotes vascular lesion formation through stimulation of smooth muscle cell proliferation and migration. *Arterioscler Thromb Vasc Biol* 2011;31:e19–e26.
19. Cui XB, Guo X, Chen SY. Response gene to complement 32 deficiency causes impaired placental angiogenesis in mice. *Cardiovasc Res* 2013;99:632–639.
20. Park ES, Choi S, Muse KN, Curry TE Jr, Jo M. Response gene to complement 32 expression is induced by the luteinizing hormone (LH) surge and regulated by LH-induced mediators in the rodent ovary. *Endocrinology* 2008;149:3025–3036.
21. Cui XB, Luan JN, Ye J, Chen SY. RGC32 deficiency protects against high-fat diet-induced obesity and insulin resistance in mice. *J Endocrinol* 2015;224:127–137.
22. Cui XB, Luan JN, Chen SY. RGC-32 deficiency protects against hepatic steatosis by reducing lipogenesis. *J Biol Chem* 2015;290: 20387–20395.
23. Tegla CA, Cudrici CD, Nguyen V, Danoff J, Kruszewski AM, Boodhoo D, *et al.* RGC-32 is a novel regulator of the T-lymphocyte cell cycle. *Exp Mol Pathol* 2015;98:328–337.
24. Luzina IG, Salcedo MV, Rojas-Pena ML, Wyman AE, Galvin JR, Sachdeva A, *et al.* Transcriptomic evidence of immune activation in macroscopically normal-appearing and scarred lung tissues in idiopathic pulmonary fibrosis. *Cell Immunol* 2018;325:1–13.
25. Reyfman PA, Walter JM, Joshi N, Anekalla KR, McQuattie-Pimentel AC, Chiu S, *et al.* Single-cell transcriptomic analysis of human lung provides insights into the pathobiology of pulmonary fibrosis. *Am J Respir Crit Care Med* 2019;199:1517–1536.
26. Liu X, Rowan SC, Liang J, Yao C, Huang G, Deng N, *et al.* Definition and signatures of lung fibroblast populations in development and fibrosis in mice and men. *bioRxiv* 2020:2020.2007.2015.203141.
27. Parimon T, Yao C, Habiel DM, Ge L, Bora SA, Brauer R, *et al.* Syndecan-1 promotes lung fibrosis by regulating epithelial reprogramming through extracellular vesicles. *JCI Insight* 2019;5:e129359.
28. Zhou Y, Zhou B, Pache L, Chang M, Khodabakhshi AH, Tanaseichuk O, *et al.* Metascape provides a biologist-oriented resource for the analysis of systems-level datasets. *Nat Commun* 2019;10:1523.
29. Bastian D, Wu Y, Betts BC, Yu XZ. The IL-12 cytokine and receptor family in graft-vs.-host disease. *Front Immunol* 2019;10:988.
30. Mizoguchi Y, Okada S. Inborn errors of STAT1 immunity. *Curr Opin Immunol* 2021;72:59–64.
31. Mirlekar B, Pylayeva-Gupta Y. IL-12 family cytokines in cancer and immunotherapy. *Cancers (Basel)* 2021;13:167.
32. Waters DW, Blokland KEC, Pathinayake PS, Burgess JK, Mutsaers SE, Prele CM, *et al.* Fibroblast senescence in the pathology of idiopathic pulmonary fibrosis. *Am J Physiol Lung Cell Mol Physiol* 2018;315: L162–L172.
33. Pedroza M, Le TT, Lewis K, Karmouty-Quintana H, To S, George AT, *et al.* STAT-3 contributes to pulmonary fibrosis through epithelial injury and fibroblast-myofibroblast differentiation. *FASEB J* 2016;30:129–140.
34. Prele CM, Yao E, O'Donoghue RJ, Mutsaers SE, Knight DA. STAT3: A central mediator of pulmonary fibrosis? *Proc Am Thorac Soc* 2012;9: 177–182.
35. O'Dwyer DN, Moore BB. Animal models of pulmonary fibrosis. *Methods Mol Biol* 2018;1809:363–378.
36. Carrington R, Jordan S, Pitchford SC, Page CP. Use of animal models in IPF research. *Pulm Pharmacol Ther* 2018;51:73–78.
37. Degryse AL, Lawson WE. Progress toward improving animal models for idiopathic pulmonary fibrosis. *Am J Med Sci* 2011;341:444–449.
38. Lee R, Reese C, Bonner M, Tourkina E, Hajdu Z, Riemer EC, *et al.* Bleomycin delivery by osmotic minipump: similarity to human scleroderma interstitial lung disease. *Am J Physiol Lung Cell Mol Physiol* 2014;306:L736–L748.
39. Luo F, Le NB, Mills T, Chen NY, Karmouty-Quintana H, Molina JG, *et al.* Extracellular adenosine levels are associated with the progression and exacerbation of pulmonary fibrosis. *FASEB J* 2016;30:874–883.
40. Sun CX, Zhong H, Mohsenin A, Morschl E, Chunn JL, Molina JG, *et al.* Role of A2B adenosine receptor signaling in adenosine-dependent pulmonary inflammation and injury. *J Clin Invest* 2006;116:2173–2182.

41. Zhou Y, Schneider DJ, Morschl E, Song L, Pedroza M, Karmouty-Quintana H, *et al.* Distinct roles for the A2B adenosine receptor in acute and chronic stages of bleomycin-induced lung injury. *J Immunol* 2011;186:1097–1106.
42. Baran CP, Opalek JM, McMaken S, Newland CA, O'Brien JM Jr, Hunter MG, *et al.* Important roles for macrophage colony-stimulating factor, CC chemokine ligand 2, and mononuclear phagocytes in the pathogenesis of pulmonary fibrosis. *Am J Respir Crit Care Med* 2007; 176:78–89.
43. Walters DM, Antao-Menezes A, Ingram JL, Rice AB, Nyska A, Tani Y, *et al.* Susceptibility of signal transducer and activator of transcription-1-deficient mice to pulmonary fibrogenesis. *Am J Pathol* 2005;167:1221–1229.
44. Kemmner S, Bachmann Q, Steiger S, Lorenz G, Honarpisheh M, Foresto-Neto O, *et al.* STAT1 regulates macrophage number and phenotype and prevents renal fibrosis after ischemia-reperfusion injury. *Am J Physiol Renal Physiol* 2019;316:F277–F291.
45. Medley SC, Rathnakar BH, Georgescu C, Wren JD, Olson LE. Fibroblast-specific stat1 deletion enhances the myofibroblast phenotype during tissue repair. *Wound Repair Regen* 2020;28:448–459.
46. Zornetzer GA, Frieman MB, Rosenzweig E, Korth MJ, Page C, Baric RS, *et al.* Transcriptomic analysis reveals a mechanism for a prefibrotic phenotype in stat1 knockout mice during severe acute respiratory syndrome coronavirus infection. *J Virol* 2010;84:11297–11309.
47. Ulloa L, Doody J, Massague J. Inhibition of transforming growth factor-beta/SMAD signalling by the interferon-gamma/STAT pathway. *Nature* 1999;397:710–713.
48. Jeong WI, Park O, Radaeva S, Gao B. STAT1 inhibits liver fibrosis in mice by inhibiting stellate cell proliferation and stimulating NK cell cytotoxicity. *Hepatology* 2006;44:1441–1451.
49. Zhu L, Qin H, Li PY, Xu SN, Pang HF, Zhao HZ, *et al.* Response gene to complement-32 enhances metastatic phenotype by mediating transforming growth factor beta-induced epithelial-mesenchymal transition in human pancreatic cancer cell line BxPC-3. *J Exp Clin Cancer Res* 2012;31:29.
50. Sun Q, Yao X, Ning Y, Zhang W, Zhou G, Dong Y. Overexpression of response gene to complement 32 (RGC32) promotes cell invasion and induces epithelial-mesenchymal transition in lung cancer cells via the NF-κB signaling pathway. *Tumour Biol* 2013;34:2995–3002.

SUPPLEMENTARY MATERIALS

to the article

"Regulator of Cell Cycle Protein (RGCC/RGC-32) Protects Against Pulmonary Fibrosis"

Irina G. Luzina, Violeta Rus, Virginia Lockatell, Jean-Paul Courneya, Brian S. Hampton, Rita Fishelevich, Alexander V. Misharin, Nevins W. Todd, Tudor C. Badea, Horea Rus, Sergei P. Atamas

SUPPLEMENTARY METHODS

Primary human lung fibroblast culture and stimulation. NHLF cultures were expanded from adult donor lungs that were intended for but ultimately not used for transplantation. Additional NHLF cultures were commercially acquired from Lonza (Walkersville, MD). Primary fibroblast cultures from patients with IPF were expanded from explant lung tissues obtained during lung transplantation surgeries. Fibroblasts were cultured in DMEM (Corning Cellgro, Manassas, VA) supplemented with 10% fetal calf serum (FCS, HyClone Laboratories, GE Healthcare Life Sciences, Logan, UT), 2 mM L-glutamine (Gemini BioProducts, West Sacramento, CA), 1 mM sodium pyruvate, MEM nonessential amino acids solution, and antibiotic-antimycotic (10,000 units/ml penicillin, 10,000 μg/ml streptomycin, and 25 μg/ml amphotericin B), all from Gibco Life Technologies (Thermo Fisher Scientific, Waltham, MA). Fibroblast cultures were maintained in T75 culture flasks (Nest Biotechnology, Rahway, NJ) in a humidified atmosphere with 5% CO2 at 37°C. Fibroblasts were passaged by washing with filtered PBS, trypsinizing with 2–5 ml 0.25% trypsin-EDTA (Gibco), and reconstituting cells in DMEM with 10% BCS before transfer to new T75 flasks, dishes, or six-well plates (Nest). In all experiments, fibroblast cell cultures were tested in passages 4 to 7. For experiments, fibroblast cultures were incubated with DMEM medium containing the same supplements and 0.5% BCS for at least 12 h before testing.

For RGCC overexpression, transfections were performed with an untagged human RGCC-encoding plasmid or noncoding vehicle control plasmid with a similar backbone, both from Origene (Rockville, MD). Transfections with recombinant plasmids were performed by electroporation using the Nucleofector II system and the Amaxa basic nucleofector kit for primary mammalian fibroblasts from Lonza. For each transfection, 0.5 – 1.0 million cells were electroporated with 1–3 μg of plasmid or using program A023 and transferred into six-well plates. Fresh media were added 18–24 h later. Cell lysates for subsequent assays, such as Western blot analysis and mRNA analysis, were collected 48 – 120 h after transfection. For all transfections with RGCC-encoding plasmids, overexpression of RGCC protein was confirmed by Western blot analysis. In some experiments, transfected cells were stimulated by recombinant human (rh) TGF-β1 (R&D Systems, Minneapolis, MN) at a concentration of 5 ng/ml in DMEM with 0.5% BCS 48 h after transfection, and cell lysates were collected 12 – 72 h later.

Acute and chronic bleomycin injury models. To model acute pulmonary inflammation and fibrosis, a single dose of 0.075 U of bleomycin (Sigma-Aldrich, St. Louis, MO), diluted in 50 ml of sterile PBS, was delivered to mouse lungs on day 0, as previously reported (1-3). Briefly, a minor anterior midline neck incision was made to make the trachea visible, a MicroSprayer (Penn-Century, Wyndmoor, Philadelphia, PA) was inserted intratracheally, and the bleomycin solution was instilled. Control mice were instilled with 50 ml of sterile PBS with no additives. On day 14 after bleomycin challenge, mice were euthanized by CO_2 asphyxiation followed by cervical dislocation. To model chronic fibrotic pathologies, repeated intraperitoneal injections of bleomycin were utilized in the chronic injury model as described (4-7) by injections 0.018 U/g of BLM or PBS (control) twice a week for 33 days. In both acute and chronic bleomycin models, bronchoalveolar lavage (BAL) samples and lung tissues were harvested immediately after euthanasia. To collect BAL samples, installation and withdrawal of 1 ml of PBS twice via an 18-gauge blunt-end needle secured in the trachea were performed in each animal. The two aliquots of BAL were pooled and centrifuged, and total and differential cell counts were performed in Giemsa-stained cytospins. Lung tissues were used for histological assessment, qRT-PCR and western blotting analyses, as well as measurements of total lung collagen.

Antibodies for western blotting. The antibodies used included anti-RGCC antibody from Novus Biologicals (Littleton, CO) (catalog no. 44450002); anti-collagen I antibody from Abcam (Cambridge, MA) (catalog no. ab138492); anti-Smad2/3 (catalog no. 8685), anti-phospho-Smad2/3 (catalog no. 8828), anti-STAT1 (catalog no. 9172), anti-phospho-STAT1 (catalog no. 7649), anti-Jak1 (catalog no. 3344), anti-STAT3 (catalog no. 4904), anti-GAPDH (catalog no. 5174), and anti-β-actin (catalog no. 4967) antibodies from Cell Signaling Technology; as well as anti-Ski (catalog no. sc-33693) and anti-SnoN (catalog no. sc-136958) antibodies from Santa Cruz Biotechnology (Dallas, TX). Secondary HRP-bound antibodies were goat anti-rabbit from EMD Millipore (Billerica, MA) (catalog no. 12–348) and goat anti-mouse from Santa Cruz Biotechnology (catalog no. sc-2005). Antibody stripping was performed using ReBlot Plus strong antibody stripping solution (EMD Millipore).

RNA-Seq procedures and analyses. The integrity and purity of the total RNA were assessed using an Agilent 2100 Bioanalyzer (Agilent, Santa Clara, CA) and a NanoDrop spectrophotometer (Thermo Scientific, Wilmington, DE). Library preparation for RNASeq was performed using the TruSeq Stranded Total Library Preparation workflow with Ribo-Zero Gold rRNA removal mix (Illumina, catalog no. 20020598), which depletes samples of both cytoplasmic and mitochondrial rRNA. Samples were processed following manufacturer's protocol. The quality, quantity, and size distribution of the Illumina library was determined using an Agilent Tapestation 2200 (Agilent, Santa Clara, CA). Short-read sequencing was performed on an Illumina HiSeq 2500, generating 100–125-bp paired-end libraries with an average of 80 million paired reads per sample. The raw RNASeq reads (fastq files) for each sample were quality controlled using FastQC software (Babraham Institute, Cambridge, UK). Quantification of transcripts was performed using Salmon v1.1.0 software in quasi-mapping-based mode (8), with subsequent summarization to gene counts using tximport v1.14.2 (9). Differential expression was analyzed using DESeq2 package of Bioconductor (10). The DESeq2-based pair-wise comparison were performed to identify genes that were differentially expressed in NHLF cultures depending on experimental conditions. The DESeq2 results were wrangled to separate up- and down-regulated genes in these pair-wise comparisons between experimental conditions, based on an arbitrarily chosen 1.5-fold change cutoff and p value ≤ 0.05. A combined table of all pair-wise comparisons was compiled and used as the input for functional enrichment analysis, which was performed using Metascape (11). Metascape was used in the express analysis mode.

SUPPLEMENTARY TABLES AND FIGURES

Supplementary Table 1. Differences in RGCC mRNA levels in fibrotic or TGF-β-stimulated tissues or cells versus control tissues or cells observed in transcriptomic profiling studies as reported in the NCBI GEO database.

Technology	GEO	Comparison	Fold diff.	Suppl. Ref.
RNA-Seq	GSE83717	IPF vs Ctrl lung tissues	-6.59	(12)
RNA-Seq	GSE73189	IPF&INSIP vs Ctrl lung tissues	-4.63	(13)
RNA-Seq	GSE52463	IPF vs Ctrl lung tissues	-2.41	(14)
RNA-Seq	GSE102674	TGF-β-treated vs Ctrl NHLFs	-1.56	(15)
RNA-Seq	GSE97829	TGF-β-treated vs Ctrl MRC5 fibroblasts	-9.41	(16)
RNA-Seq	GSE119007	TGF-β-treated vs Ctrl NHLFs	-1.41	(17)
RNA-Seq	GSE134692	IPF&ALI vs Ctrl lung tissues	-1.23	(18)
Microarray	GSE40839	SSc-ILD vs Ctrl lung fibroblasts	-2.52	(19)
Microarray	GSE40266	TGF-β-treated vs Ctrl ovarian fibroblasts	-3.61	(20)
Microarray	GSE17708	TGF-β-treated vs Ctrl A549 cell line	-1.44	(21)
Microarray	GSE2705	TGF-β-treated vs Ctrl lamina cribrosa cells	-1.97	(22)

Abbreviations: ALI, acute lung injury; Ctrl, control; ILD, interstitial lung disease; INSIP, idiopathic nonspecific interstitial pneumonia; IPF, idiopathic pulmonary fibrosis; SSc-ILD, systemic sclerosis-associated interstitial lung disease.

Supplementary Table 2. Top differentially expressed genes in NULL-transfected and TGF-β-stimulated (NULL+TGF-β), compared to NULL-transfected non-stimulated (NULL), NHLF6 and NHLF8 cultures, based on RNA-Seq (NULL+TGF-β vs NULL) comparison.

name	log2Fold	pvalue	name	log2Fold	pvalue
IL11	6.9	1.26E-69	RSC1A1	-6.4	2.70E-03
IL24	-8.9	1.84E-08	WAPAL	-6.0	1.72E-03
COL10A1	7.4	5.84E-10	RASL11A	-3.6	1.55E-13
TGIF2-C20orf24	8.5	5.40E-07	NOL7	-4.2	7.94E-05
PAGR1	8.5	8.03E-06	HK2	-4.3	1.13E-04
MDFI	8.3	5.98E-06	DES	-6.2	3.35E-03
GMEB2	8.1	3.18E-06	RP5-1021I20.4	-5.8	2.27E-03
SIK1	7.8	3.99E-05	SORBS2	6.4	5.11E-03
KCTD21	7.4	5.10E-05	ALDH1A3	6.5	5.81E-03
PANX2	7.4	1.16E-04	PMEPA1	3.6	1.35E-08
DACT3	5.3	1.99E-09	FBLN7	-5.0	2.71E-03
ZNF844	-6.8	7.18E-05	FAT3	3.7	8.06E-06
PTHLH	4.9	5.30E-10	ANKRD32	-6.0	5.81E-03
ELN	4.5	3.37E-22	RELN	-3.5	8.39E-07
C2orf44	-5.1	2.51E-08	GLTP	-4.6	1.80E-03
OLFM2	4.3	1.01E-13	CTNNBL1	-3.8	1.80E-04
SENP8	-7.3	5.83E-04	C10orf11	-5.0	5.68E-03
GMPR	-6.6	2.17E-04	MGME1	-3.6	4.10E-05
IFITM10	7.0	8.43E-04	SNX30	4.7	4.26E-03
SLC16A6	-4.7	8.76E-07	ZNF700	-6.2	9.84E-03
CLDN14	4.1	4.32E-09	DCPS	5.8	9.04E-03
IGFBP3	4.0	2.03E-11	HTR7	-3.7	1.84E-04
AMIGO2	3.8	2.53E-24	LINC01410	-3.8	3.36E-04
FAM196A	-6.4	2.96E-04	RP5-907D15.4	3.3	3.25E-05
LRRC17	3.9	1.05E-11	SYBU	-4.7	6.26E-03
NUF2	6.6	1.36E-03	FICD	3.8	1.15E-03
SUSD3	6.6	1.67E-03	KIAA1279	-3.3	1.12E-04
DIO3	6.4	8.44E-04	GUCY1B3	-4.8	8.41E-03
FAM127A	7.2	3.62E-03	SPTLC3	-4.1	3.91E-03
WNT7B	7.0	3.10E-03	PCDH1	3.3	1.38E-04
LIPG	6.4	1.64E-03	PCDH19	4.1	7.06E-03
SEMA7A	3.7	1.10E-20	RP11-567M16.1	4.4	9.74E-03
MFN1	-5.5	1.81E-04	TMOD1	4.1	7.30E-03
EGR2	5.9	3.44E-04	EVI2A	-3.8	4.60E-03
LINC01583	5.6	2.89E-04	NPL	-3.7	3.69E-03
IDO1	-3.7	4.74E-12	PTGES	-3.9	7.78E-03
COL8A2	-4.0	4.62E-07	DACT1	3.6	4.23E-03
BOP1	4.3	4.08E-05	SLC39A8	-3.9	8.87E-03
KRT80	4.8	1.75E-04	PRPF18	-3.9	8.78E-03
LRRC32	3.9	2.08E-07	AP003419.11	3.6	6.80E-03
CNN1	4.1	1.56E-05	ST8SIA5	3.7	9.09E-03
COL7A1	3.5	6.02E-28	LINC01085	-3.3	7.05E-03
UBE2D1	-5.8	1.06E-03	GIN1	-3.4	8.62E-03

Supplementary Table 3. Top differentially expressed genes in RGCC-overexpressing (RGCC) compared to NULL-transfected (NULL) NHLF6 and NHLF8 cultures based on RNA-Seq (RGCC vs NULL) comparison.

name	log2Fold	pvalue	name	log2Fold	pvalue
RGCC	9.0	5.29E-19	ZNF699	6.3	1.06E-03
CH507-254M2.1	-9.3	9.22E-09	PLA2G4B	4.5	5.20E-04
TGIF2-C20orf24	8.0	2.73E-06	FICD	4.0	4.30E-04
ARSI	-7.8	7.23E-07	GS1-114I9.3	6.6	2.97E-03
DSTYK	-8.2	5.58E-06	DACT3	3.6	6.18E-05
GMEB2	7.9	5.31E-06	FAT3	3.4	1.89E-05
HJURP	-7.1	1.03E-04	TEC	-6.9	7.27E-03
CH17-258A22.4	-7.5	4.40E-04	TUBB3	-7.0	8.68E-03
GH1	5.5	2.56E-31	IFITM10	6.4	2.43E-03
RP11-542C16.2	7.7	1.39E-03	ASPM	-6.5	4.18E-03
PANX2	6.7	5.73E-04	TCEAL8	-3.3	8.39E-05
RPS3AP5	-6.8	1.20E-03	PRKCQ	6.5	4.46E-03
AFG3L2	-4.2	2.54E-06	PINK1	-3.9	8.34E-04
VPS37D	-6.9	1.96E-03	NPIPA2	6.4	3.21E-03
KCNJ2	6.7	1.47E-03	CLN3	3.6	5.97E-04
KCTD21	6.4	4.50E-04	HYAL1	6.4	5.37E-03
AC098823.3	6.5	9.29E-04	UBE2D1	-4.0	1.51E-03
NINL	-4.8	1.40E-04	GABARAPL2	3.7	2.27E-03
POLH	-5.6	3.41E-04	ZNF630	-6.3	9.37E-03
CDC25C	-6.6	1.41E-03	GPAA1P2	-4.0	7.42E-03
H2AFZ	-3.6	1.31E-07	GSTM5	-3.7	5.44E-03
RBAK	-6.8	2.31E-03	NCAPG2	-4.0	1.05E-02
ARID2	-4.2	2.91E-04	C15orf59	-3.3	3.68E-03
EML6	6.7	2.98E-03	PHF5A	3.4	4.50E-03
CLGN	-7.0	5.22E-03	LRRC8C	-3.5	9.32E-03
HS3ST2	6.5	1.51E-03			

Supplementary Table 4. Top differentially expressed genes in RGCC-overexpressing and TGF-β-stimulated (RGCC+TGF-β), compared to NULL-transfected with no additional stimulation (NULL), NHLF6 and NHLF8 cultures, based on RNA-Seq (RGCC+TGF-β vs NULL) comparison.

name	log2Fold	pvalue	name	log2Fold	pvalue
RGCC	9.5	8.27E-21	TUBB3	-7.7	3.90E-03
HOXA4	-8.4	2.31E-07	EEPD1	-5.8	7.63E-04
TGIF2-C20orf24	8.6	4.34E-07	TEC	-7.6	3.13E-03
FBXL17	-8.2	1.45E-06	PMEPA1	3.5	1.90E-08
COL10A1	7.4	5.45E-10	IGFBP3	3.5	5.45E-09
RP11-305M3.2	-7.7	1.84E-05	RP4-756H11.5	-7.5	3.71E-03
IL11	5.8	6.43E-50	KLHL12	-4.4	5.85E-04
LMNB1	-6.8	6.95E-10	SLC14A1	-3.4	6.97E-07
WNT16	-7.6	4.16E-05	KPNA7	6.5	2.82E-03
GH1	5.6	3.47E-32	NPIPA2	6.4	2.74E-03
CYP1B1	-7.6	1.08E-04	BAIAP2L1	-5.6	2.05E-03
NTN4	-7.3	3.95E-05	SLC19A2	5.2	1.98E-03
HPSE	-7.4	5.96E-05	TNFRSF8	-6.9	6.74E-03
FAN1	-7.2	3.49E-05	TMEM87B	-3.7	2.13E-04
F2RL2	-8.1	6.76E-04	TRAPPC11	-4.6	1.55E-03
AMIGO2	4.5	2.49E-33	PBK	-4.7	1.77E-03
LPCAT1	-5.3	2.56E-09	IFITM1	3.7	1.26E-04
ZC2HC1A	-7.5	2.16E-04	TPRG1L	6.9	8.91E-03
RP11-21J18.1	-7.8	1.38E-03	PCDH19	4.6	2.53E-03
GMEB2	6.9	7.21E-05	TMEM144	-3.7	7.09E-04
CLDN14	4.4	2.82E-10	ITGA4	-4.0	1.69E-03
NPHP3-ACAD11	7.6	1.10E-03	ARAP2	-6.0	7.70E-03
ARID2	-5.7	3.23E-06	PCDH1	3.3	1.21E-04
SMIM11	-5.0	4.27E-07	CIT	-3.7	1.41E-03
PAGR1	6.9	3.32E-04	SPTLC3	-3.9	2.25E-03
RASL11A	-3.8	2.97E-16	SC5D	-3.3	5.01E-04
LHX4-AS1	-4.2	2.67E-09	CCDC34	-3.8	2.55E-03
POLH	-6.0	8.12E-05	MSH2	4.3	7.32E-03
CLGN	-7.7	2.15E-03	DACT1	3.8	2.90E-03
CDK1	-6.6	2.23E-04	TTF2	-3.4	1.40E-03
NIPAL2	-5.1	2.76E-05	ZDHHC13	-3.5	2.49E-03
RP11-373L24.1	-7.0	9.80E-04	RAB11FIP2	-3.9	9.89E-03
GPC6	-7.2	1.23E-03	FICD	3.4	2.53E-03
AC006011.4	-7.1	1.21E-03	ZNF684	-3.5	2.69E-03
PTHLH	4.0	2.34E-07	MAPT	-3.6	5.42E-03
CPEB2	-4.3	6.35E-07	ABCC6	-3.7	1.07E-02
QPRT	-4.5	4.72E-06	GIN1	-3.5	4.88E-03
LRRC17	3.7	2.33E-10	CPM	-3.6	7.66E-03
SIK1	6.4	6.95E-04			

Supplementary Table 5. Top differentially expressed genes in RGCC-overexpressing and TGF-β-stimulated (RGCC+TGF-β), compared to NULL-transfected and TGF-β-stimulated (NULL+TGF-β), NHLF6 and NHLF8 cultures, based on RNA-Seq (RGCC+TGF-β vs NULL+TGF-β) comparison.

name	log2Fold	pvalue	name	log2Fold	pvalue
RGCC	12.0	1.18E-14	RP11-262H14.4	-3.5	1.16E-06
HOXA4	-9.7	1.54E-09	CIT	-4.5	1.32E-04
FAN1	-8.7	4.82E-07	KLHL12	-4.7	1.94E-04
IL24	8.0	4.09E-07	HZGJ	6.1	2.96E-03
AGGF1	-8.6	1.77E-06	POLH	-5.1	1.06E-03
LMNB1	-7.2	7.33E-11	SLC18B1	5.9	1.98E-03
FBXL17	-7.8	4.69E-06	COL8A2	3.5	7.21E-06
RP11-305M3.2	-7.4	3.87E-05	CPEB2	-3.6	5.88E-05
PEX11B	7.8	1.69E-04	CA9	-5.9	2.97E-03
NTN4	-7.0	7.78E-05	LPCAT1	-3.6	9.13E-05
SNORA16A	-11.2	4.49E-04	NFKBIE	-4.8	9.03E-04
GH1	5.7	4.38E-31	ABCB10	-5.9	4.89E-03
RP11-61N20.3	-7.2	1.77E-04	LINC01410	3.8	2.13E-04
QPRT	-5.8	1.57E-09	RHEBP2	6.1	7.97E-03
ZNF844	6.5	1.18E-04	NPIPA2	5.9	5.93E-03
ARID2	-5.8	4.03E-06	KIAA1279	3.3	1.35E-04
SP4	7.0	3.34E-04	PANX2	-4.7	1.85E-03
HPSE	-7.0	1.81E-04	BTBD11	-5.0	4.75E-03
GAREML	-7.1	3.74E-04	SMAP2	-5.3	5.06E-03
MATN3	-7.2	6.49E-04	CDK1	-5.1	4.95E-03
PRDM6	-7.2	1.19E-03	ITGA4	-3.9	1.84E-03
CD200	-6.3	1.79E-04	BZRAP1	-3.9	1.49E-03
GMPR	6.4	3.58E-04	UBE2D1	4.9	5.69E-03
SMIM11	-4.8	1.44E-06	CCNA1	4.9	5.68E-03
RP5-1021I20.4	6.6	5.07E-04	KCNMB3	4.0	3.59E-03
FAM196A	6.3	3.61E-04	AATF	5.1	9.42E-03
WAPAL	6.4	7.65E-04	RP11-221J22.1	4.9	8.17E-03
KRT80	-4.9	7.21E-05	ZNF35	3.9	4.93E-03
AC006011.4	-7.0	1.35E-03	ZNF391	3.5	2.23E-03
WDR60	-4.7	5.30E-06	ETNK1	-3.6	4.47E-03
RHEBP1	-7.1	2.25E-03	NCBP1	-3.3	3.00E-03
PPA1	4.2	7.32E-06	SUSD6	-4.6	1.00E-02
ZNF654	-7.0	2.53E-03	DTL	-4.4	9.54E-03
BAIAP2L1	-5.9	1.03E-03	PRPF18	3.8	8.92E-03
CTC-471J1.8	-7.3	5.55E-03	MAPT	-3.5	7.25E-03
MGME1	3.9	7.43E-06	MYCT1	3.4	7.34E-03

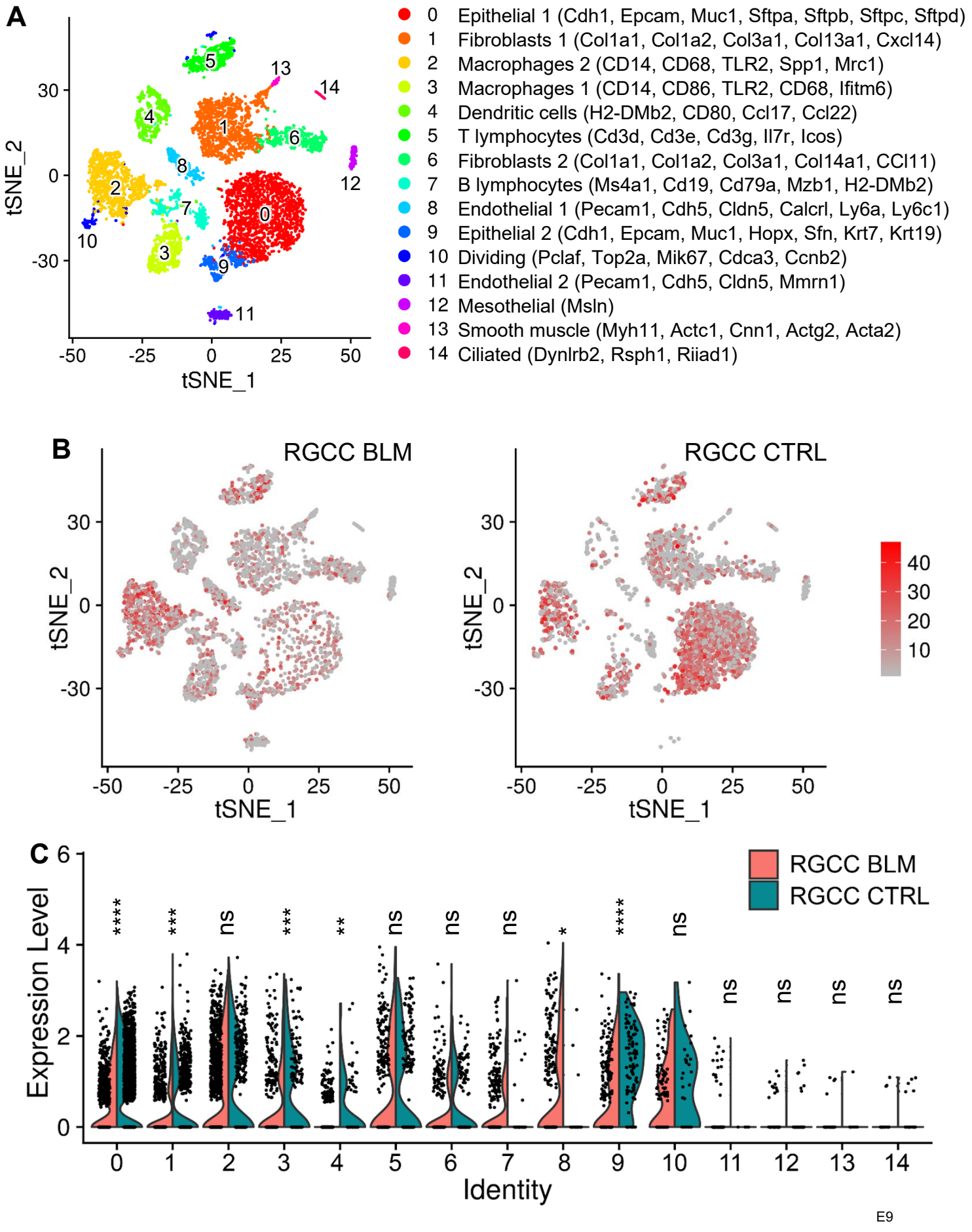
A
0 Epithelial 1 (Cdh1, Epcam, Muc1, Sftpa, Sftpb, Sftpc, Sftpd)
1 Fibroblasts 1 (Col1a1, Col1a2, Col3a1, Col13a1, Cxcl14)
2 Macrophages 2 (CD14, CD68, TLR2, Spp1, Mrc1)
3 Macrophages 1 (CD14, CD86, TLR2, CD68, Ifitm6)
4 Dendritic cells (H2-DMb2, CD80, Ccl17, Ccl22)
5 T lymphocytes (Cd3d, Cd3e, Cd3g, Il7r, Icos)
6 Fibroblasts 2 (Col1a1, Col1a2, Col3a1, Col14a1, CCl11)
7 B lymphocytes (Ms4a1, Cd19, Cd79a, Mzb1, H2-DMb2)
8 Endothelial 1 (Pecam1, Cdh5, Cldn5, Calcrl, Ly6a, Ly6c1)
9 Epithelial 2 (Cdh1, Epcam, Muc1, Hopx, Sfn, Krt7, Krt19)
10 Dividing (Pclaf, Top2a, Mik67, Cdca3, Ccnb2)
11 Endothelial 2 (Pecam1, Cdh5, Cldn5, Mmrn1)
12 Mesothelial (Msln)
13 Smooth muscle (Myh11, Actc1, Cnn1, Actg2, Acta2)
14 Ciliated (Dynlrb2, Rsph1, Riiad1)
tSNE_1
tSNE_2
B
RGCC BLM
RGCC CTRL
40
30
20
10
C
RGCC BLM
RGCC CTRL
Expression Level
Identity
**** *** ns *** ** ns ns ns * **** ns ns ns ns ns

Supplementary Figure 1. Analysis of RGCC expression in the lung cells of bleomycin (BLM)-challenged and control (CTRL) mice using a publicly available single-cell RNA-Seq dataset GSE131800 (23). Seurat 4.0 software (https://satijalab.org/seurat/) was used for analyses. All code used to perform these analyses is available on GitHub at https://github.com/j-p-courneya/RGCC-in-GSE131800. **A.** t-SNE plot of combined samples, with cluster identities assigned based on selective expression of indicated genes. **B.** Feature plot of RGCC expression levels of RGCC BLM-challenged (left) and control (right) mice. **C.** Split violin plot of RGCC expression by cell cluster. Statistical significance of differences in mean RGCC expression between bleomycin-challenged and control mice is indicated for each cluster: ns $p > 0.05$, *$p <= 0.05$, **$p <= 0.01$, ***$p <= 0.00$, ****$p <= 0.0001$.

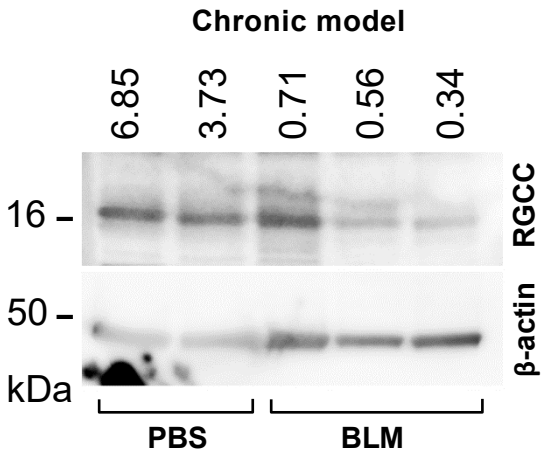

Supplementary Figure 2. Western blotting of cultured primary mouse lung fibroblasts for RGCC and β-actin. Lungs were extracted postmortem from PBS- or bleomycin-treated mice in the chronic bleomycin challenge model and mechanically dissociated. The dissociated tissues were cultured in DMEM for fibroblast outgrowth. The established primary fibroblast cultures were passaged 4 times and used for this analysis.

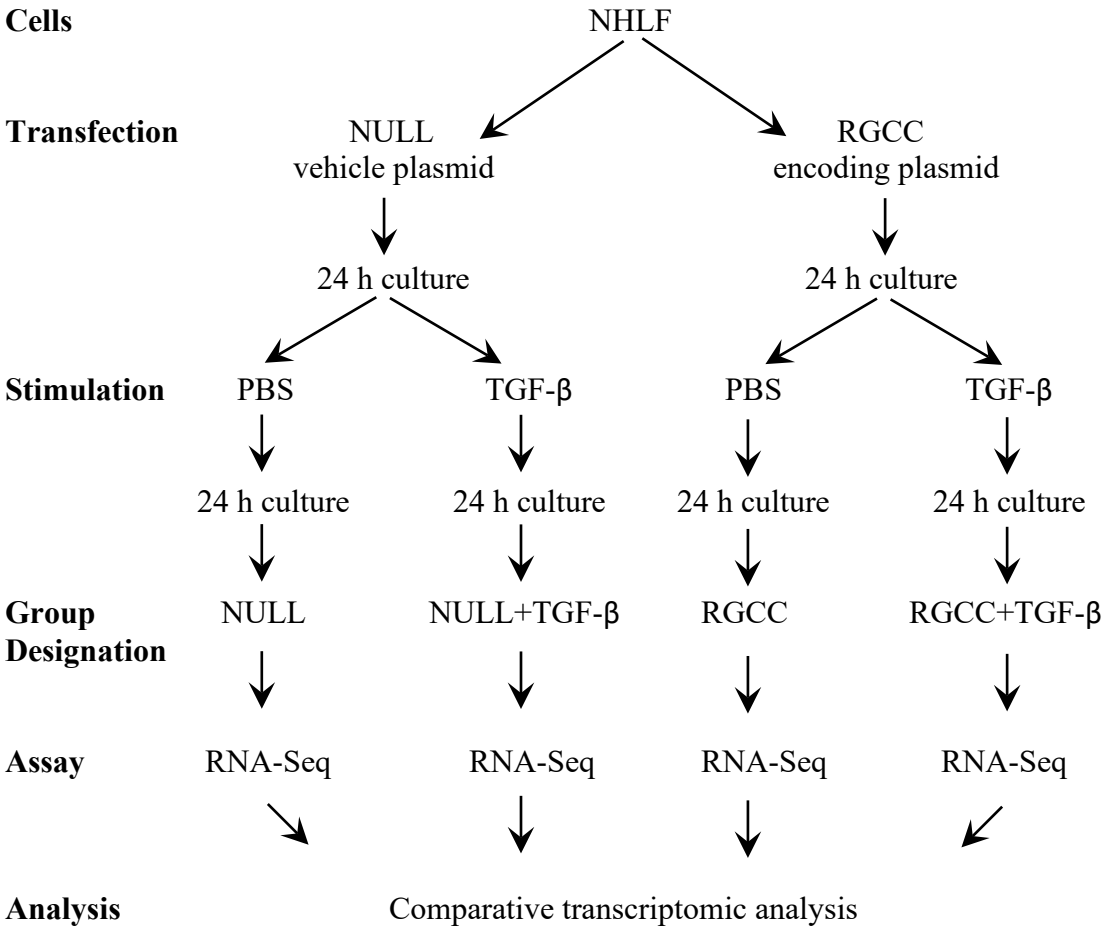

Supplementary Figure 3. Experimental setup of the RNA-Seq-based transcriptomic profiling of RGCC-overexpressing NHLF6 and NHLF8.

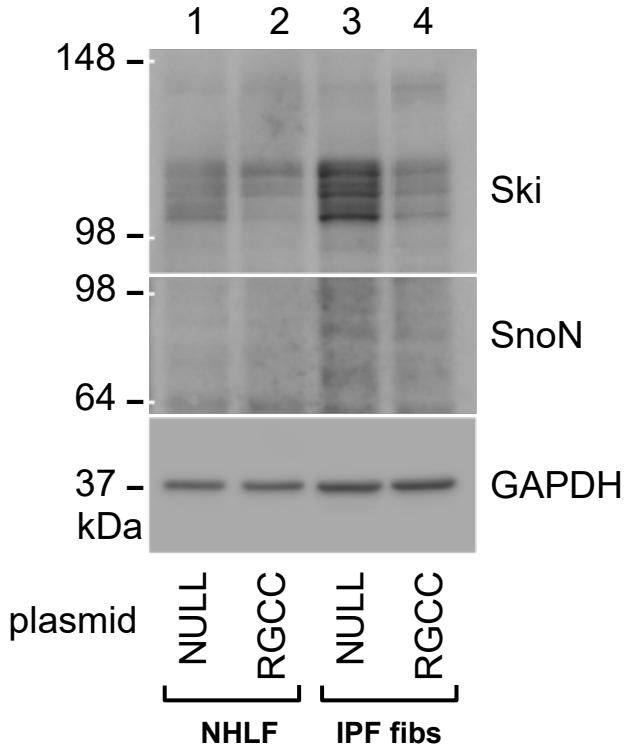

Supplementary Figure 4. Effect of RGCC overexpression on Ski and SnoN protein expression in NHLFs and IPF-derived fibroblasts transfected with either non-coding NULL or RGCC-encoding plasmids. Repeated once in separate NHLF and IPF fibroblast cultures from different donors, with similar results.

SUPPLEMENTARY REFERENCES

1. Pochetuhen K, Luzina IG, Lockatell V, Choi J, Todd NW, Atamas SP. Complex regulation of pulmonary inflammation and fibrosis by ccl18. *Am J Pathol* 2007;171(2):428-437.
2. Luzina IG, Kopach P, Lockatell V, Kang PH, Nagarsekar A, Burke AP, Hasday JD, Todd NW, Atamas SP. Interleukin-33 potentiates bleomycin-induced lung injury. *Am J Respir Cell Mol Biol* 2013;49(6):999-1008.
3. Luzina IG, Lockatell V, Todd NW, Kopach P, Pentikis HS, Atamas SP. Pharmacological in vivo inhibition of s-nitrosoglutathione reductase attenuates bleomycin-induced inflammation and fibrosis. *J Pharmacol Exp Ther* 2015;355(1):13-22.
4. Sun CX, Zhong H, Mohsenin A, Morschl E, Chunn JL, Molina JG, Belardinelli L, Zeng D, Blackburn MR. Role of a2b adenosine receptor signaling in adenosine-dependent pulmonary inflammation and injury. *J Clin Invest* 2006;116(8):2173-2182.
5. Baran CP, Opalek JM, McMaken S, Newland CA, O'Brien JM, Jr., Hunter MG, Bringardner BD, Monick MM, Brigstock DR, Stromberg PC, et al. Important roles for macrophage colony-stimulating factor, cc chemokine ligand 2, and mononuclear phagocytes in the pathogenesis of pulmonary fibrosis. *Am J Respir Crit Care Med* 2007;176(1):78-89.
6. Zhou Y, Schneider DJ, Morschl E, Song L, Pedroza M, Karmouty-Quintana H, Le T, Sun CX, Blackburn MR. Distinct roles for the a2b adenosine receptor in acute and chronic stages of bleomycin-induced lung injury. *J Immunol* 2011;186(2):1097-1106.
7. Lee R, Reese C, Bonner M, Tourkina E, Hajdu Z, Riemer EC, Silver RM, Visconti RP, Hoffman S. Bleomycin delivery by osmotic minipump: Similarity to human scleroderma interstitial lung disease. *Am J Physiol Lung Cell Mol Physiol* 2014;306(8):L736-748.
8. Patro R, Duggal G, Love MI, Irizarry RA, Kingsford C. Salmon provides fast and bias-aware quantification of transcript expression. *Nat Methods* 2017;14(4):417-419.
9. Soneson C, Love MI, Robinson MD. Differential analyses for rna-seq: Transcript-level estimates improve gene-level inferences. *F1000Res* 2015;4:1521.
10. Love MI, Huber W, Anders S. Moderated estimation of fold change and dispersion for rna-seq data with deseq2. *Genome Biol* 2014;15(12):550.
11. Zhou Y, Zhou B, Pache L, Chang M, Khodabakhshi AH, Tanaseichuk O, Benner C, Chanda SK. Metascape provides a biologist-oriented resource for the analysis of systems-level datasets. *Nat Commun* 2019;10(1):1523.
12. Vukmirovic M, Herazo-Maya JD, Blackmon J, Skodric-Trifunovic V, Jovanovic D, Pavlovic S, Stojsic J, Zeljkovic V, Yan X, Homer R, et al. Identification and validation of differentially expressed transcripts by rna-sequencing of formalin-fixed, paraffin-embedded (ffpe) lung tissue from patients with idiopathic pulmonary fibrosis. *BMC Pulm Med* 2017;17(1):15.
13. Yu X, Gu P, Huang Z, Fang X, Jiang Y, Luo Q, Li X, Zhu X, Zhan M, Wang J, et al. Reduced expression of bmp3 contributes to the development of pulmonary fibrosis and predicts the unfavorable prognosis in iip patients. *Oncotarget* 2017;8(46):80531-80544.

14. Nance T, Smith KS, Anaya V, Richardson R, Ho L, Pala M, Mostafavi S, Battle A, Feghali-Bostwick C, Rosen G, et al. Transcriptome analysis reveals differential splicing events in ipf lung tissue. *PLoS One* 2014;9(3):e92111.

15. Selvarajah B, Azuelos I, Plate M, Guillotin D, Forty EJ, Contento G, Woodcock HV, Redding M, Taylor A, Brunori G, et al. Mtorc1 amplifies the atf4-dependent de novo serine-glycine pathway to supply glycine during tgf-beta1-induced collagen biosynthesis. *Sci Signal* 2019;12(582).

16. Savary G, Dewaeles E, Diazzi S, Buscot M, Nottet N, Fassy J, Courcot E, Henaoui IS, Lemaire J, Martis N, et al. The long noncoding rna dnm3os is a reservoir of fibromirs with major functions in lung fibroblast response to tgf-beta and pulmonary fibrosis. *Am J Respir Crit Care Med* 2019;200(2):184-198.

17. Mukherjee S, Sheng W, Michkov A, Sriarm K, Sun R, Dvorkin-Gheva A, Insel PA, Janssen LJ. Prostaglandin e2 inhibits profibrotic function of human pulmonary fibroblasts by disrupting ca(2+) signaling. *Am J Physiol Lung Cell Mol Physiol* 2019;316(5):L810-L821.

18. Sivakumar P, Thompson JR, Ammar R, Porteous M, McCoubrey C, Cantu E, 3rd, Ravi K, Zhang Y, Luo Y, Streltsov D, et al. Rna sequencing of transplant-stage idiopathic pulmonary fibrosis lung reveals unique pathway regulation. *ERJ Open Res* 2019;5(3).

19. Lindahl GE, Stock CJ, Shi-Wen X, Leoni P, Sestini P, Howat SL, Bou-Gharios G, Nicholson AG, Denton CP, Grutters JC, et al. Microarray profiling reveals suppressed interferon stimulated gene program in fibroblasts from scleroderma-associated interstitial lung disease. *Respir Res* 2013;14:80.

20. Yeung TL, Leung CS, Wong KK, Samimi G, Thompson MS, Liu J, Zaid TM, Ghosh S, Birrer MJ, Mok SC. Tgf-beta modulates ovarian cancer invasion by upregulating caf-derived versican in the tumor microenvironment. *Cancer Res* 2013;73(16):5016-5028.

21. Sartor MA, Mahavisno V, Keshamouni VG, Cavalcoli J, Wright Z, Karnovsky A, Kuick R, Jagadish HV, Mirel B, Weymouth T, et al. Conceptgen: A gene set enrichment and gene set relation mapping tool. *Bioinformatics* 2010;26(4):456-463.

22. Kirwan RP, Leonard MO, Murphy M, Clark AF, O'Brien CJ. Transforming growth factor-beta-regulated gene transcription and protein expression in human gfap-negative lamina cribrosa cells. *Glia* 2005;52(4):309-324.

23. Parimon T, Yao C, Habiel DM, Ge L, Bora SA, Brauer R, Evans CM, Xie T, Alonso-Valenteen F, Medina-Kauwe LK, et al. Syndecan-1 promotes lung fibrosis by regulating epithelial reprogramming through extracellular vesicles. *JCI Insight* 2019;5.